

Optimization of Al-doped ZnO nanorods for photovoltaic applications



By

Rafi Ullah

(128-FBAS/MSPHY/F12)

Supervisor

Dr. Muhammad Mumtaz

Assistant professor

Department of physics, FBAS

IU Islamabad

Co-supervisor

Dr. Muhammad Sultan

Senior Scientific Officer NS&CD

National Centre for Physics

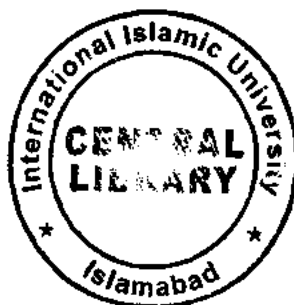
Quaid-i-Azam University, Islamabad

Department of Physics

Faculty of Basic and Applied Sciences

International Islamic University Islamabad

(2015)



Accession No TH-14827 (K) 9/9

MS
621.381542
RAO

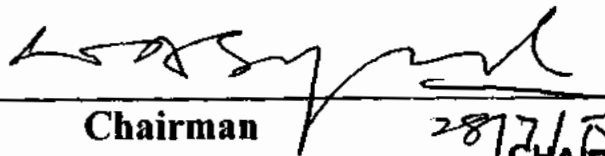
- Photovoltaic Cells
- Al-doped ZnO nanorods
- Doping
u

Optimization of Al-doped ZnO nanorods for photovoltaic applications

by
Rafi Ullah

(128-FBAS/MSPHY/F-12)

This thesis submitted to department of physics International Islamic University Islamabad for the award of Ms Physics degree.



Chairman

Department Of Physics

International Islamic university Islamabad

28/7/15
CHAIRMAN
DEPT. OF PHYSICS
International Islamic University
Islamabad



Dean

Faculty of Basic and Applied Sciences

International Islamic University Islamabad

Final Approval

It is certified that the work presented in this thesis entitled “**Optimization of Al-doped ZnO nanorods for photovoltaic applications**” by Rafi Ullah , Registration No: 128-FBAS/MSPHY/F12 is of sufficient standard in scope and quality for the award of degree of MS Physics from the Department of Physics, International Islamic University Islamabad Pakistan.

Viva Voce Committee

Chairman _____
(Department of Physics)

Supervisor _____

Co-supervisor _____

External Examiner _____

Internal Examiner _____

بِسْمِ اللَّهِ الرَّحْمَنِ الرَّحِيمِ

DEDICATED

**TO
MY LOVING PARENTS**

**BROTHERS, SISTERS
RESPECTED TEACHERS**

**AND MY CUTE
M.ASNAF AND M.SALIH**

Declaration

I Rafi Ullah (Registration No: 128-FBAS/MSPHY/F12), Student of MS Physics (session 2012-2014), hereby declare that the material presented in the thesis entitled "**Optimization of Al-doped ZnO nanorods for photovoltaic applications**" is my own work and has not been published or submitted as research work or thesis in any other university or institute in Pakistan or abroad.



Rafi Ullah

(128-FBAS/MSPHY/F-12)

Date: _____

Forwarding Sheet by Research Supervisor

The thesis entitled "**Optimization of Al-doped ZnO nanorods for photovoltaic applications**" submitted by Rafi Ullah (Registration No: 128-FBAS/MSPHY/F12) in the partial fulfillment of MS degree in Physics has been completed under my guidance and supervision. I am satisfied with the quality of his research work and allow him to submit this thesis for further process to graduate with Master of Science degree from the Department of Physics, as per IIU Islamabad rules and regulation.



Dr. Muhammed Mumtaz,
Assistant Professor
Department of Physics,
International Islamic University,
Islamabad.

Date: 07-07-2015

Acknowledgment

My foremost acknowledgment is to that unseen power that governs all the affairs of nature and mans the almighty Allah, because it was due to the blessing of him that I could complete my research work successfully. At the same time I offer my humble words of thanks and gratitude to the towering personality to the Holy Prophet (PBUH) fountain of light, guidance and knowledge to all human beings.

With deep sense of gratitude, I wish to express my sincere thanks to my supervisor of this research work **Dr. Muhammad Mumtaz** and co-supervisor **Dr. Muhammad Sultan** for their excellent guidance and support throughout the work. I received very useful and excellent academic training from them. I can never forget the kindness behavior of my supervisor.

I am also grateful to my friends **Hamaun Khattak**, **Engg. Abdul Majid**, **Mir Azam Khan**, **Fawad Khan** and my younger brother **Naveed Ullah**, and elder brother **Sir Daraz Khan** for their encouragement and kind support extended towards me.

Last but not the least I am very thankful to my batch mates, **Pindora group**, and all my class fellows especially **Abid Zaman**, **Jaffer Saddique Abdul Mateen**, for their immense cooperation without them my stay here would not have been memorable.

Finally, I would like to share this moment of happiness with my parents, **Brothers**, **Sisters** and all of my family members for their continuous love and support. I offer my heartiest words of thanks to my beloved **Papa Sir Anjam Khan (Late)**.

Rafi Ullah

Table of Contents

Chapter 1	1
Introduction and Literature review	1
1.1 Nanotechnology and applications	1
1.2 Synthesis approaches to Nanotechnology	1
1.2.1 Top-down approach	1
1.2.2 Bottom-up approach	1
1.3 Metal Oxides	2
1.4 Introduction to Zinc Oxide (ZnO)	3
1.4.1 Crystal structure of ZnO	3
1.4.2 Basic properties of ZnO	4
1.4.3 ZnO nanostructures	5
1.5 Doping in ZnO	6
1.5.1 n-type doping	6
1.5.2 p-type doping	6
1.5.3 Incorporation of Aluminum (Al)	6
1.6 ZnO nanostructure applications	7
1.7 Literature review.....	8
1.7.1 Growth parameters.....	8
1.7.1.1 Pre-treatment of substrate	8
1.7.1.2 Pre-coating surfaces.....	8
1.7.1.3 Annealing temperature of seed layer.....	9
1.7.1.4 Annealing time of seed layer.....	9
1.7.1.5 Precursor concentration.....	9
1.7.1.6 Solution pH.....	9
1.7.1.7 Growth temperature.....	10
1.7.1.8 Growth time.....	10
1.8 Physical mechanism for ZnO nanorods growth.....	10
1.9 Reaction mechanism	11
1.10 Motivation.....	13

References.....	14
Chapter 2	18
Characterization Techniques	18
2.1 X-Ray Diffraction (XRD).....	18
2.1.1 X-rays.....	19
2.1.2 Bragg's Law.....	19
2.1.3 Crystal size determination.....	20
2.2 UV/Visible Spectroscopy.....	20
2.2.1 Working principle of UV/Visible Spectrometer.....	21
2.3 Scanning Electron Microscopy.....	22
2.4 Energy Dispersive Spectroscopy	23
References	25
Chapter 3	27
Experimental and Synthesis	27
3.1 Pulsed Laser Deposition Method	27
3.2 Chemical Vapour Deposition Method	27
3.3 Magnetron Sputtering Method	28
3.4 Vapour Phase Technique	28
3.5 Chemical Bath Deposition (CBD) Method	29
3.5.1 Advantages of CBD Method	29
3.6 Experimental	30
3.6.1 Material used	30
3.6.2 Substrate cleaning	30
3.6.3 Seed solution	31
3.6.4 Preparation of ZnO seed by spin coating method	31
3.6.5 Synthesis of Al-doped ZnO nanorods	31
References	35
Chapter 4	37
Results and Discussion	37
4.1 XRD results.....	37

4.2 Optical results	40
4.2.1 Energy band gap	40
4.2.2 Transmittance	42
4.3 optimization of nanorods	44
4.4 Compositional Analysis	49
4.5 Conclusions	51
References	52

List of Figures

Figure 1.1 Top-down and Bottom up approaches of Nanotechnology	2
Figure 1.2 Hexagonal wurtzite crystal structure of ZnO	4
Figure 1.4 Possible incorporation of Al ³⁺ ions into the Zincite lattice	7
Figure 1.5 ZnO nanorods mechanism	11
Figure 2.1 Graphical representation of Bragg's law	19
Figure 2.2 Experimental arrangements for UV/Visible Spectrometer	21
Figure 2.3 Scanning Electron Microscope construction	22
Figure 2.4 Working principle of EDX	24
Figure 3.1 Substrates cleaning steps	30
Figure 3.2 Al-doped ZnO nanorods solution (a) Top view (b) Side view	32
Figure 3.3 Flow chart for Al-doped ZnO nanorods solution	34
Figure 4.1 XRD pattern of Undoped, 0.5 wt.%, 1.0wt.%, 2.0wt.% and 4.0wt.% Al-doped ZnO nanorods.....	38
Figure 4.2 Average crystallite size variations with different Al concentration.....	39
Figure 4.3 Energy band gap of undoped ZnO nanorods from DRS spectra.....	41
Figure 4.4: Plots of $[F(R_{\infty})/hv]^2$ vs. hv shows K-M transferred reflectance spectra of 0.5 wt.%, 1.0 wt.%, 2.0 wt.% and 4.0 wt.% Al-doped ZnO nanorods.....	42
Figure 4.5 Transmittance spectra of Undoped and 0.5 wt.%, 1.0 wt.%, 2.0 wt.%, 4.0 wt.% Al-doped ZnO nanorods.....	43
Figure 4.6 Combined optical transmittance graph of undoped and 0.5 wt.%, 1.0 wt.%, 2.0 wt.%, 4.0 wt.% Al-doped ZnO nanorods.....	44
Figure 4.7 Variety of Al-doped ZnO nanorods.....	45
Figure 4.8 SEM image of Al-doped ZnO nanorods grown on uncoated glass substrate.....	46
Figure 4.9: SEM image of Al-doped ZnO nanorods grown on ZnO seed coated (6-times) glass substrate.....	47
Figure 4.10 SEM image of Al-doped ZnO nanorods grown on 10-times ZnO seed coated glass substrate.....	48
Figure 4.11: Al-doped ZnO nanorods grown on (a) uncoated (b) 4-times (c) 8-times (d) 12-times ZnO seed coated substrates.....	49
Figure 4.12: EDX spectra of 0.5 wt.% Al-doped ZnO nanorods	50

Figure 4.13: EDX spectra of 1 wt.% Al-doped ZnO nanorods50

List of Tables

Table 1.1 Physical properties of Zinc Oxide	4
Table 3.1 A series of samples with different precursor concentration ratios	32
Table 4.1 Average crystallite size of undoped and Al-doped ZnO nanorods.....	39
Table 4.2 Band gap values of undoped and Al-doped ZnO nanorods	43

Abstract

One dimensional (1-D) nanostructured semiconductors have attracted attention of scientific community due to their excellent electronic and optoelectronic properties. ZnO is one of the most important semiconductor material that can be grown in a wide range of morphologies such as nanorods, nanowires, nanorings, which can play a key role in future nanodevices. ZnO has already been used in thin film solar cells as electron collector. In future generation heterostructure based solar cells nanostructured ZnO can play important role for enhanced photo-absorption and charge carrier separation if well aligned nanostructures are used. Here a variety of ZnO nanorod structures were grown by tuning the experimental conditions and their optimum parameters are reported in this thesis.

Chemical bath deposition (CBD) method was used to synthesize one dimensional ZnO nanorod structures. As Al doping in ZnO enhances the device efficiency in thin film solar cells. Here we systematically prepared a variety of Al-doped ZnO nanorods by varying the growth parameters of CBD method. The grown samples were investigated with the help of different techniques. The X-ray diffraction (XRD) pattern showed that the grown nanorods have wurtzite crystal structure along c-axis. The ZnO nanorods exhibited highest transmittance almost 92% with 2wt. % Al doping and also its band gap has been increased with Al doping. The surface morphology of these nanorods studied using scanning electron microscope (SEM) showed that the nanorods have hexagonal morphology with random alignment on the substrate. For compositional analysis Energy dispersive spectroscopy (EDX) was carried out.

To improve the alignment and size distribution of nanorods, a variety of experimental conditions were tested and their effect on growth was analyzed. Moreover the seed layer was optimized for controlling the morphology of nanostructures. It was found that the number of seed layer coatings play key role to control the diameter, density and alignment of the nanorods. This observation is very essential to control the growth of the nanorods on any substrate. Finally, well aligned nanorod with controlled density and diameter were achieved by carefully controlling the growth parameters.

Chapter No: 1**Introduction and Literature review****1.1 Nanotechnology and applications**

Nanotechnology is simply the exploitation of nanomaterials with structural feature in between those of atoms and their bulk. In other words its definition can be made that it is the technology of designations and applications of nanomaterials with new properties. The nanoscale dimensions materials are different in properties from those of atoms as well as bulk materials. The nanomaterials have opened up possible way for new innovative efficient devices [1-2]. Currently, nanotechnology has much more applications in the field of science and technology including medical applications, biomedical applications, energy production and conversion applications, energy storage, aerospace, healthcare, infrastructure, security purposes, food safety and agricultures [3-6]. In short, nanotechnology provides fast response, long life time and applied in every aspect of our modern life.

1.2 Synthesis approaches of nanotechnology

To investigate and explore the physical and chemical properties of nanomaterials its synthesis is the primary foremost step. In general nanotechnology uses two main approaches.

- Top-down approach
- Bottom-up approach

1.2.1 Top-down approach

Top-down approach is a method that slashing down bigger building blocks into smaller pieces till their constitution size reach to nanoscale level. In this technique larger component of material is converted into its smaller segment [7]. Different synthesis techniques of this approach are Ball milling method, Lithography method, fabrication by embossing and nano fabrication by skiving.

1.2.2 Bottom-up approach

In bottom-up approach smaller constituents (atoms and molecules) combined together and form complex assembly of nanomaterials. This approach is just copy of nature. This approach is easier than the above one. Many synthesis techniques of this approach are used to

build nanomaterials [8]. Some of these are Sol-gel method, hydrothermal method, Chemical vapour deposition (CVD), Co-precipitation method, Chemical bath deposition (CBD) etc. The diagrammatical representation of these two approaches is illustrated in figure 1.1.

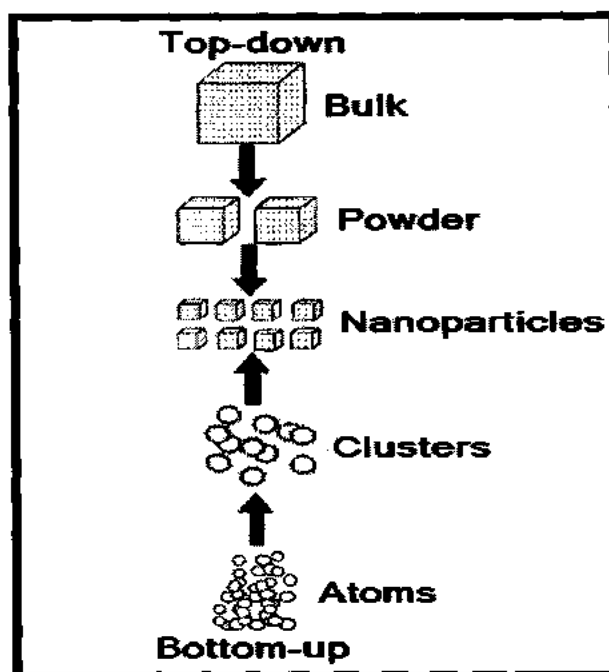


Figure 1.1: Top-down and bottom-up approaches of nanotechnology [12].

1.3 Metal Oxides

Metal oxides are crystalline solid material with metal cation and oxygen anion. The reaction of metal elements with oxygen can make different metal oxide compound [9]. Some of the well-known oxides are Copper oxide, Iron oxide, Carbon oxide, Zinc oxides etc. The reaction of metal oxide with water causes basis, but when they react with acids then they form salts. Usually their grain size lies in the micro-meter range and they are believed as particles because of greater size. The nano-meter scale metal oxides have much more applications compared to other conventional metal oxides in the field of material science. The manufacturing of fine scale metal oxides in nanometer range is not too much easy [10]. Up to certain limited number metal oxides have small grain size and also lie in the nanometer range. At nano scale they show different properties than their bulk. The most significant use of metal oxide is to use them as a semiconductor [11].

1.4 Introduction to Zinc Oxide (ZnO)

Zinc oxide (ZnO) is an n-type direct band gap semiconductor. In the past decade global research interest in the wide band gap semiconductor material has been focused towards ZnO which possess invaluable properties like large free exciton binding energy of 60 meV at room temperature, band gap 3.37 eV, high carrier mobility, high thermal conductivity, and high visible light transparency [12-15]. It is a soft material and its band gap can be tuned with doping to advance its properties. It is inexpensive, non-hazardous and easily obtainable in nanostructure form which make it suitable for wide range of applications. More than a few research groups tried to improve its nanostructure synthesis in order to get good quality ZnO and to use it further in solar cell, thermoelectronics [16-19], lasing, sensing, optical wave guide and many other optoelectronic devices [20-21]. It belongs to the family of transparent conductive oxide because it operates in the UV wavelength. ZnO has vast technological importance because of its exclusive optical and electrical properties.

1.4.1 Crystal structure of ZnO

ZnO naturally prefer stable hexagonal wurtzite crystal structure in which each ion of Zn^{2+} (cation) bounded tetrahedrally to four O^{2-} ions (anions) and vice versa. The lattice parameters of ZnO hexagonal unit cell are $a=b= 3.249\text{\AA}$ and $c=5.2059\text{\AA}$ with a density of 5.60g cm^{-3} . The value of c/a ratio is about 1.602 while for an ideal hexagonal structure it is 1.633. So it is slightly different from an ideal value. This kind of tetrahedral arrangement of Zn^{2+} and O^{2-} stack alternatively along c-axis. There is simple polar symmetry along c-axis which is responsible for the piezoelectricity in ZnO. In ZnO structure the oppositely charged ions produces stable Zn terminated (0001) and O terminated (000 $\bar{1}$) polar face along c-axis. The cation or anion terminated surfaces leads ZnO to have negatively or positively charged surfaces [22]. The difference in electronegativity values of Zn^{2+} and O^{2-} resulting to a strong ionic character between Zn^{2+} and O^{2-} . The wurtzite structure is thermodynamically stable phase under ambient condition [23].

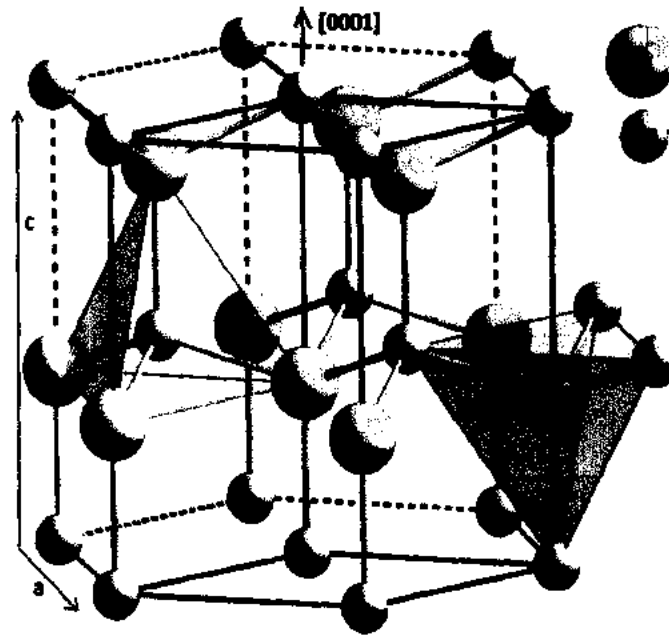


Figure 1.2: Hexagonal wurtzite crystal structure of ZnO [23-24]

1.4.2 Basic properties of ZnO

Table 1.1 Physical properties of Zinc Oxide.

Molecular Formula	ZnO
Molar Mass	81.408 g/mol
Odor	Odorless
Appearance	White
Lattice	Hexagonal
Lattice Parameters a, c	0.325, 0.5207 nm
Structure	Wurtzite
Density	5.606 g/cm ³
Solubility in Water	0.16mg/100ml (30 °C)
Melting Point	1975 °C
Boiling Point	2360 °C
Band gap	3.37 eV
Refractive index (n _D)	2.0041
Thermal conductivity (K)	69 , 60⊥ Wm ⁻¹ K ⁻¹
Thermal expansion coefficient (α)	2.92 , 4.75⊥10 ⁻⁶ /K

1.4.3 ZnO nanostructures

Nanotechnology deals with the materials at nanometer scale (ranging from 1nm to 100nm). It is the most emerging progressive technology which gives idea about a very small size particle and also has unfathomable relation to other fields of science and engineering. Physical and chemical properties of nanomaterials are relatively different from their bulk form. Their physical properties specially depend upon the types of compounds, defects in the lattice, bond types and impurities added [25]. The charges and electrons have confined behavior within a nanostructure causes discrete energy level. Due to this confinement behavior, nanomaterials have wide band gap as compared to the bulk semiconductor. The quantum confinement in bulk materials is smaller while much larger in nanostructure material, which results structural distortion because of large number of dangling bonds [26]. Furthermore the structural properties (particle size and inter atomic spacing) affect the surface energy, surface area and optical properties of the material. The surface energy, surface area and band gap decreases when the particle size increases and vice versa [27]. With the decrease in particle size the band gap increases which lead it to the inter-band transition promoting to a higher frequency. Besides the above characteristics, the emissions from nanostructure semiconductor material can be tuned by varying the nanostructure size. One dimensional nanostructure materials play a very crucial role in the rapid progress of the fields of natural sciences. The polar charges distribution and the structure arrangement in ZnO is in such a way to minimize the electrostatic energy, which is the main responsible force that compel the growth to polar surface dominated nanostructure. Due to this effect ZnO nanostructure grow in unusual various forms such as nanobelts [28], nanohelices, nanosprings [29-31], nanorings [32], nanorods, nanowires [33], nanocombs [34] and nanocages as shown in the figure 1.2. Its nanostructure can be grown on different substrates like glass, FTO, ITO silicon and sapphire. In the past few years, ZnO nanorods have received great focusing in the research field due to their high surface to volume ratio and improving electron transportation speed inside the organic and inorganic hybrid solar cells [35-36].

1.5 Doping in ZnO

Doping is a procedure of adding some foreign atoms into the host material. The impurity atoms are called dopants. Recently this study has received considerable attention. The main aim of doping is to alter some of the desirable properties of the host material. It is an effective way of optimizing electrical conductivity, Optical and magnetic properties. A large area of work has been investigated on doping ZnO with different elements. The group III elements (Ga, In, Al) can easily substitute Zn in crystal lattice. Such doping has been exhibited high carrier concentration more than 10^{20} cm^{-3} [37].

1.5.1 n-type doping

According to the widely known concept ZnO naturally exhibits n-type conductivity because of high concentration of intrinsic donor defects such as V_{O} and Zn_{i} , is large in ZnO. It's very easy to obtain n-type ZnO semiconductor by doping different impurity materials like group III elements and traditional metals (Pb, Fe, Mg, Ni, Co) in ZnO lattice [38]. These dopants contribute an electron and form shallow donor level in ZnO.

1.5.2 p-type doping

In p-type ZnO, electron is accepted by the dopant from the host material while creating a positive hole. Unlike n-type, fabrication of p-type ZnO is not only complicated but also a challenging problem. These difficulties have many reasons including the ZnO tendency towards p-type conductivity is low while n-type is high, self-compensation effect arises from Zn_{i} and V_{O} in the native ZnO [39]. Group-I and group-V elements can create deep acceptors in ZnO [37].

1.5.3 Incorporation of Al

To improve the electronic properties of the host materials it is needed that the dopant ion to be incorporated into the crystal structure. The ion will either go to the lattice sites or will incorporate interstitially. In case of Al as a dopant and ZnO as a host material the electrical conductivity of ZnO is almost certainly improved if the Al^{+3} ions occupy Zn^{+2} lattice site because it offers a free electron. Charged defects are definitely produced when Al^{+3} occupies the Zn^{+2} site. The representation of Zn^{+2} site occupied by Al^{+3} is shown in a very simple way in the below figure 1.3 (a).

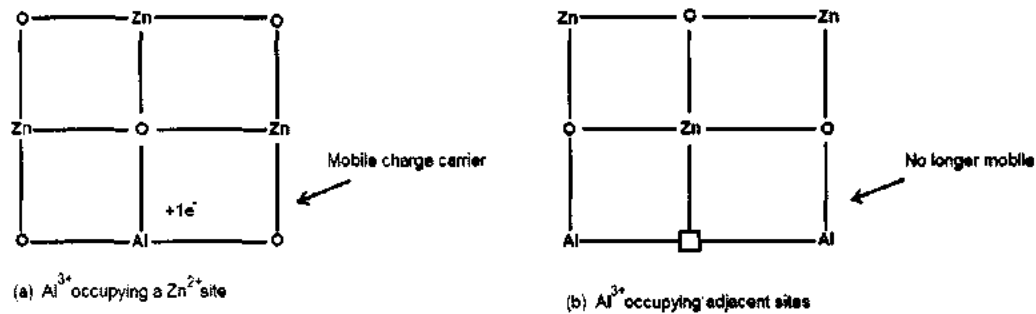


Figure 1.4: Possible incorporation of Al^{3+} ions into the Zincite lattice.

Quantum chemical approach has been explained the increase in the n-type electrical conductivity of ZnO with Al doping [40]. To obtain the most favorable performance, the allocation of dopant ions would be in the correct sites of the host material also the incorporation of the dopant ions would be uniform and homogeneous up to a certain limiting value of concentration. At high concentration the dopant ions may possibly go to occupy the adjacent or proximal lattice sites. Such type of incorporation can generate ion vacancies, producing neutral defects. Neutral defects have no contribution in the conductivity of the material [41]. The occupation of dopant ions at proximal sites are shown in the figure 1.3 (b).

The conductivity of the host material ZnO is enhanced with Al doping at the condition of donor behavior from Al. The Al has one valence electron greater than Zn. So when it substitute Zn atom or occupy the interstitial sites, then the concentration of charge carriers increases in the material. For ZnO, the dopant Al is preferred because of smaller difference in the electronegativity values of Zn (1.65) and Al (1.61). While the second reason is that, in both the tetrahedral and octahedral configurations ionic radii of Al (0.530, 0.675 Å) are smaller than that of Zn (0.60, 0.710 Å) that's why Al can easily substitute into the Zn lattice site [42].

1.6 ZnO nanostructure applications

- ZnO nanorods and nanowires can detect change in electrical current when pass through it. So they are used in gas sensors and have a potential for detecting NO_2 , CO, H_2 , etc [43-45]
- It is possibly investigated that ZnO biosensors based nanostructure can be used for the detection of biological molecule. 1D ZnO biosensors have been obtained in limited number.

- To advance the suitable option for renewable energy, ZnO films frequently used as a transparent front contact of the solar cell and LCDs [46].
- ZnO nanotubes have applications in white light emitting diodes. Besides this, it is considered suitable for space technology because of radiation resistance property [47].
- It can also be used as an additive and conductive thin film in other various products including thin film batteries.
- Very recently, ZnO nanorods and nanowires have been utilizing in Field effect transistors and inter-molecular junction diodes ultraviolet photodetectors [48-50].

1.7 Literature review

A short summary of the imperative reports presented by Y. Tao et al. [51], M. Guo et al. [52], T. Ma et al. [53], Q. Li et al. [54] belonging to the effects of different growth parameters on the morphology, orientation and alignment, crystal quality, density, diameter and length of ZnO nanorods. Any of the parameters have own effect on the resultant ZnO nanorods.

1.7.1 Growth parameters

1.7.1.1 Pretreatment of substrate

On the basic principle of hydrothermal process it is believed that at certain saturation ratio in the solution, heteronucleation onto a substrate easily occur then a homogeneous nucleation. The hurdle to homogenous nucleation is the surface energy of forming a smaller nucleus. On the other hand, formation of heteronucleation is easier but its controlling is not easy. It has been found that the alignment of nanorods on pre-coated substrate is more than on uncoated substrate. Pre-coating the substrate with nanoparticles can control the orientation of nanorods to a great extent. This is because of matching lattice structure and also due to the dipole moment which try to align itself with charged ZnO seed to minimize energy.

Polarity of ZnO influences the morphology of ZnO nanostructure. ZnO nanorods cannot be grown on O-terminated surfaces because these surfaces help two dimensions (2D) growth. Thus only Zn-terminated surfaces are responsible for ZnO nanorods or nanowires growth [52].

1.7.1.2 Pre-coating surfaces

The thickness of the seed layer is one of the important parameter which controls the density of the nanorods. But on the other hand it has some effect on the orientation of nanorods. The orientation becomes poor when the thickness of the seed layer decreases. The reason is

that, at nanoscale the substrate is not smooth enough and will definitely be unable to align all those planes of the particles which are parallel to the substrates. So, due to the decreasing thickness of the seed layer and roughness of the substrate at the nano level, the nanorods of ZnO merge and grow together.

1.7.1.3 Annealing temperature of seed layer

With the high annealing temperature, changes may occur in the crystal seed size and its quality. The annealing temperature plays an imperative role in the crystal seed quality and its size. At elevated temperature, the interaction among the particles increases, the particles stick together, and finally they form a bigger ZnO island. The seed shows hexagonal morphology in the temperature range of 600 °C to 700 °C, while at 300 °C the seed appearance is small nanoparticles.

1.7.1.4 Annealing time of seed layer

The crystallinity and size of the nanoparticles are influenced by the annealing time, but this effect is limited compared to annealing temperature. Size and crystallinity can be improved with increasing annealing time.

1.7.1.5 Precursor concentration

The concentration of the reactants in the growth solution is the most important and fundamental parameter which affects the diameter distribution of the grown nanorods, but the relation between precursor concentration and diameter of nanorods is not linear. Certainly, with the precursor concentration, the diameter of the nanorods can be controlled to a certain extent, but still the role of the pre-deposited ZnO seed layer cannot be ignored, because the pre-deposited seed has a pivotal role in diameter distribution. The diameter of the nanorods reduces and slims down with decreasing concentration.

1.7.1.6 Solution pH

The pH of the solution has some remarkable effects on the diameter and crystal phase of ZnO nanorods grown on a substrate. Aligned ZnO nanorods of wurtzite structure can be obtained in the basic region of pH (ranging from 9 to 13). It has been reported that the diameter of the nanorods decreases exponentially with the pH of the growth solution. For aligned ZnO nanorods, the suitable value of pH is above 10 [51-54].

1.7.1.7 Growth temperature

It has been observed that ZnO nanorods can be grown at different temperature. During the ZnO nanorods growth, the reaction temperature also has a little impact on the length of nanorods and its optical properties. With increasing reaction temperature or growth temperature, both length and UV emission of ZnO nanorods increases while green emission is inverse to the growth temperature.

1.7.1.8 Growth time

In the very beginning, the growth rate is very slow, because in early stages deposition occurs in the radial direction to form nano-crystalline grains of ZnO (hexagonal structure). After some time, the axial growth rate (growth in the direction perpendicular to the substrate) rapidly increases while the growth in radial direction decreases. In-short the immersion time does not affect the morphology of ZnO nanorods but highly affect the aspect ratio.

1.8 Physical mechanism for ZnO nanorods growth

X. Y. Kong [55] and Z. L. Wang [56] reported that in a typical Wurtzite structure, the polar nature surfaces of ZnO are responsible for 1D ZnO nanorods growth because they are charged either positively or negatively. So they have tendency to attract ions of opposite charge like Zn^{+2} or OH^{-1} . Due to this attraction of opposite charges, the ions will try to cover up the surfaces and will react to form ZnO. In this way the nanorods continuously grow layer by layer and will acquire good alignment. Furthermore, the nanorods grow along (0001) direction, perhaps the dipole moment along this direction.

Pacholskie et al. [57] reported that smaller nanoparticles come close together and combined to form larger dimension. They also put forward the concept that thin diameter nanorods of ZnO grow in the initial stage of growth. Eventually, these individual bundles stick together, form rods of larger diameter to reduce the surface energy. It has been suggested that at high concentration of the reactants the nucleation of ZnO will be fast and large number of ZnO nuclei will be form. Then these nuclei start to aggregate because of extra high saturation and each of them will rise up separately into rod like crystal structure. Finally, their structural designs are like flower

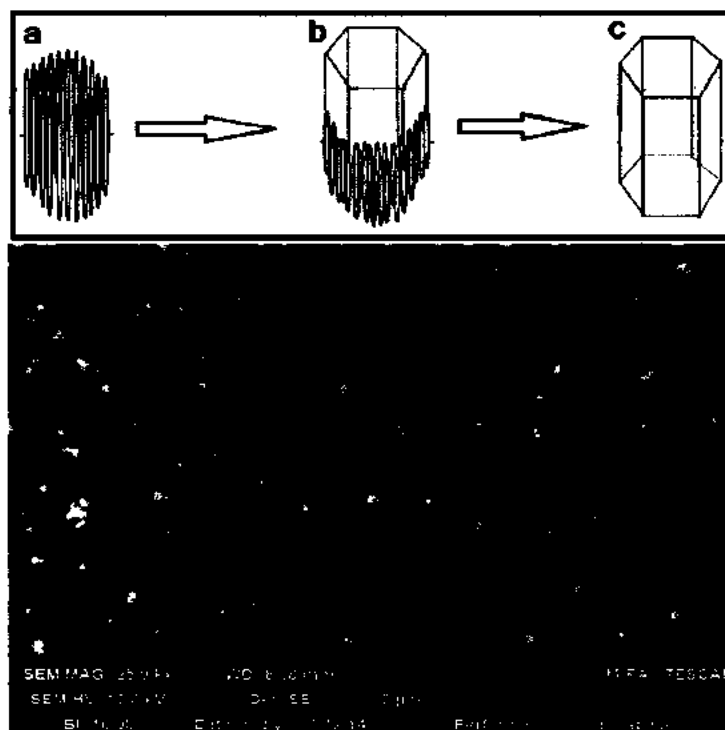
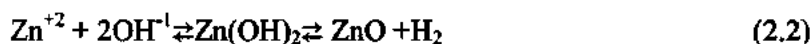
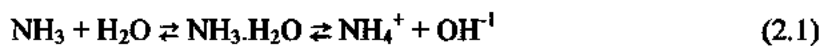


Figure 1.5: ZnO nanorods mechanism.

1.9 Reaction mechanism

It is believed that the following chemical reactions are involved in the synthesis of ZnO nanorods [58-59].



The ammonia act as a pH buffer, form ammonium hydroxide and provide OH^- ions while the decomposition of Zinc acetate provides Zn^{+2} ions. These ions may form a variety of nonnumeric hydroxyl i.e. $\text{Zn}(\text{OH})^+$, $\text{Zn}(\text{OH})_2$, $\text{Zn}(\text{OH})_3^-$ and $\text{Zn}(\text{OH})_4^{2-}$. After that, these species dehydrated at the surface of seed layer and construct solid ZnO nuclei. The coordination of ammonia in ZnO crystalline growth is to obstruct growth at certain faces. Thus, the length and growth of rods is promoted along the c-axis or Zn terminated polar planes with continues supply of opposite ions (Zn^{+2} , OH^-).

C. H. Hsu and D. H. Chen[60] synthesized Al-doped ZnO nanorods by using chemical bath deposition approach with an average diameter of about 64.7 ± 16.8 nm, and an average length of $1.0 \mu\text{m}$. They obtained maximum conductivity at Al/Zn molar ratio of about 3.7%. The conductivity was enhanced approximately 1000 times while at that molar ratio the electrical resistivity value was about $6.4 \times 10^{-4} \Omega\text{cm}$. Moreover, they showed some good results of transmittance spectra of ZnO nanorods array in the visible region. But with Al doping the increase in transmittance was not more significant.

1.10 Motivation

Solar cell is one of the most efficient electronic applications of renewable energy approach where photon energy is converted directly into desired electrical energy by photovoltaic effect. Recently, due to reports on global warming and energy needs it gaining great attention day by day. It is the cleanest source of energy. Moreover, in many remote areas where electricity is unavailable due to high cost but solar irradiation is plentiful there. Electricity can be utilized in those remote areas by using solar cell (photovoltaic) technology.

The main aim of the present work is well aligned ZnO nanorods by using chemical bath deposition (CBD) method. Next, to study its structural, optical and morphological properties with aluminum doping at nano level. Doping with certain metals electronic structure of ZnO can be tuned. This variation in the electronic structure can bring changes in its electrical, optical and magnetic properties. Aluminum is preferred as a dopant because with the addition of Al atom into ZnO matrix as an impurity enhances several properties of ZnO to some extent. Secondly its ionic radius is smaller than zinc and also offers one free electron.

Furthermore, the second reason is the exploration of one dimensional ZnO nanorods in solar cell. In third generation heterostructure based solar cells metal oxide nanorods can be used as electron/hole collector for more efficient solar cells. Well aligned ZnO nanorods provide shorter, direct and ordered path for the collection of the photoexcited charge carriers and reduces the recombination losses.

References

- [1] M. C. Roco, C. A. Mirkin, M. C. Hersam, Nanotechnology research directions for societal needs in 2020: summary of international study, *J Nanopart Res* **13**(3), 897(2011).
- [2] C. N. R. Rao, A. Muller, A. K. Cheetham, *The Chemistry of Nanomaterials*, WILEYVCH Verlag GmbH & Co. KGaA, Weinheim, page 1(2004).
- [3] P. Boisseau, and B. Loubaton, Nanoscience and nanotechnologies: hopes and concerns nano-medicine, nanotechnology in medicine, *C. R. Physique* **12**, 620 (2011).
- [4] L. A. DeLouise, Applications of nanotechnology in dermatology, *Journal of Investigative Dermatology* **132**, 964 (2012).
- [5] S. K. Arora, R. W. Foley, J. Youtie, P. Shapira, and A. Wiek, Drivers of technology adoption- the case of nanomaterials In building construction, *Technological Forecasting & Social Change* **87**, 232 (2014).
- [6] S. Chattopadhyay, L. C. Chen, and K. H. Chen, Energy production and conversion applications of one-dimensional semiconductor nanostructures, *NPG Asia Mater.* **3**(6), 74 (2011).
- [7] T. Harper, *J. American Chemical Society.* **81**, 14 (2003).
- [8] Levins, Christopher, Schafmeister, Christian, *J. Cheminform.* **37**, 5 (2006).
- [9] N. Greenwood, A. Earnshaw, *Chemistry of Elements*, 2nd Edition, Oxford: Butterworth-Heinemann Publisher, (1997).
- [10] K. Bandyopadhyay, *J. Materials Science.* **21**, 16 (1981)
- [11] C. T. Kresge, M. E. Leonowicz, W. J. Roth, J. C. Vartuli, J. S. Beck, *J. Nature.* **359**, 710 (1992).
- [12] M. Willander, O. Nur, Q. X. Zhao, L. L. Yang, M. Lorenz, B. Q. Cao, J. Z. Pérez, C. Czekalla, G. Zimmermann, M. Grundmann, A. Bakin, A. Behrends, M. A. Suleiman, A. E. Shaer, A. C. Mofor, B. Postels, A. Waag, N. Boukos, A. Trvalos, H. S. Kwack, J. Guinard, and D. L. S. Dang, *Nonotechnology* **20**, 332001 (2009).
- [13] S. Kim, M. S. Kim, K. G. Yim, G. Nam, D. Y. Lee, J. S. Kim, J. S. Kim, J. S. Son, and J. Y. Leem, *J. Korean Phys.Soc.* **60**, 1599 (2012).
- [14] R. C. Pawar, J. S. Shaikh, S. S. Suryavanshi, and P. S. Patil, *Curr. Appl. Phys.* **12**, 778 (2012).
- [15] R. C. Pawar, H. S. Kim, and C. S. Lee, *Scripta Mater.* **68**, 142 (2013).

- [16] E. Fortunato, A. Goncalves, A. Marques, A. Viana, H. Aguas, L. Pereira, I. Ferreira, P. Vilarinho, R. Martins, *Surf. Coat. Technol.* **20**, 180 (2004).
- [17] A. Tubtimtae and M. W. Lee, *Superlattices. Microstruct.* **52**, 987 (2012).
- [18] H. Yang, J. S. Lee, S. Bae, and J. H. Hwang, *Curr. Appl. Phys.* **9**, 797 (2009).
- [19] T. H. Fang and S. H. Kang, *J. Phys. D: Appl. Phys.* **41**, 245303 (2008).
- [20] P. Yu, Z. K. Tang, G. K. L. Wong, M. Kawasaki, A. Ohtomo, H. Koinuma, Y. Segawa, *J. Cryst. Growth*, **601**, 184 (1998).
- [21] C. Jagadish and S. J. Pearton, *Zinc oxide bulk, thin films and nanostructures*. Amsterdam: Elsevier. 1st ed. (2006).
- [22] Z. L. Wang, ZnO nanowire and nanobelt platform for nanotechnology, *Materials Science and Engineering R* **64**, 33 (2009).
- [23] H. Morkoc and U. Ozgur, *General properties of ZnO, Zinc Oxide: Fundamentals, materials and device technology*, WILEY-VCH Verlag, 1 (2009).
- [24] C. Klingshirn, ZnO: Material, physics and applications, *ChemPhysChem* **8**, 782 (2007).
- [25] C. Litton, D. Reynolds, and T. Collins, *Zinc oxide materials for electronic and optoelectronic device applications*. 1st ed. Hoboken: Wiley. (2011).
- [26] G. C. Yi, *Semiconductor nanostructures for optoelectronic devices*. 1st ed. Heidelberg: Springer (2012).
- [27] A. Stwertka, *A guide to the elements*. 1st ed. New York: Oxford University Press (2002).
- [28] Z. W. Pan, Z. R. Dai, and Z. L. Wang, *Science* **291**, 1947 (2001).
- [29] X. Y. Kong and Z. L. Wang, *Nano Letters* **3**, 1625 (2003).
- [30] P. M. Gao, Y. Ding, W. J. Mai, W. L. Hughes, C. S. Lao, Z. L. Wang, *Science* **309**, 1700 (2005).
- [31] P. X. Gao, W. J. Mai, and Z. L. Wang, *Nano Letters* **6**, 2536 (2006).
- [32] X. Y. Kong, Y. Ding, R. Yang, Z. L. Wang, *Science* **303**, 1348 (2004).
- [33] W. J. Mai, P. X. Gao, C. S. Lao, *Chemical Physics Letters* **460**, 253 (2008).
- [34] C. S. Lao, P. M. Gao, R. S. Yang, Y. Zhang, Y. Dai, Z. L. Wang, *Chemical Physics Letters* **417**, 358 (2006).
- [35] K. Yu and J. H. Chen, *Enhancing Solar Cell Efficiencies through 1-D Nanostructures Nanoscale*, *Res. Lett.* **4**, 1 (2009).
- [36] Z. L. Wang, *Nanostructures of zinc oxide Mater. Today* **7**, 26 (2004).

- [37] A. Janotti, C. G Van de Walle, Fundamentals of zinc oxide as a semiconductor. Reports on Progress in Physics, **72(12)**, 126501 (2009).
- [38] U. Ozgur, Y. I. Alivov, C. Liu, A. Teke, M. A. Reshchikov, S. Dogan, V. Avrutin, S.J. Cho, and H. Morkoc, A comprehensive review of ZnO materials and devices. Journal of Applied Physics, **98(4)**, 041301 (2005).
- [39] H. Morkoc, and U. Ozgur, Zinc oxide fundamentals, materials and device technology. Weinheim: Wiley-VCH 1sted (2009).
- [40] F. Maldonado and A. Stashans, Al-doped ZnO; Electronic, electrical and structural properties. Journal of Physics and Chemistry of Solids, **71(5)**, 784(2010).
- [41] H. Serier, M. Gaudon, and M. Mntrier, Al-doped ZnO powdered materials; Al solubility limit and IR absorption properties, Solid State Sciences, **11(7)**, 1192(2009).
- [42] A. E. Jimenez-Gonzalez, A. Jose, S. Urueta, and R. Suarez-Parra, Optical and electrical characteristics of aluminum-doped ZnO thin films prepared by solgel technique. Journal of Crystal Growth, **192(3-4)**, 430(1998).
- [43] P. S. Cho, K. W. Kim, and J. H. Lee, NO₂ sensing characteristics of ZnO nanorods prepared by hydrothermal method. Journal of Electroceramics, **17**, 975 (2006).
- [44] H. Gong, J.Q. Hu, J. H. Wang, C. H. Ong, F. R. Zhu, Nano-crystalline Cu doped ZnO thin film gas sensor for CO. Sensors and Actuators B: Chemical, **115**, 247(2006).
- [45] C. S. Rout, A.R. Raju, A. Govindaraj, C. N. R. Rao, Hydrogen sensors based on ZnO nanoparticles. Solid State Communications, **138**, 136 (2006).
- [46] K. Ellmer, A. Klein, and B. Rech. Transparent conductive zinc oxide: basics and applications in thin film solar cells. Springer series in materials science. Springer, Berlin, (2008).
- [47] K. Hembram, D. Sivaprahasam, T. N. Rao, J. Euro Ceramic Society. **31**, 1905 (2011).
- [48] M. S. Arnold, P. Avouris, Z. W. Pan, Z. L Wang, Field-effect transistors based on single semiconducting oxide nanobelts. J. Phys. Chem. B **107**, 659 (2003).
- [49] C. H. Liu, W. C. Yiu, F.C.K. Au, J. X. Ding, C. S. Lee, S. T. Lee. Electrical properties of zinc oxide nanowires and intramolecular p-n junctions. Appl. Phys. Lett. **83**, 3168 (2003).
- [50] S. E. Ahn, J. S. Lee, H. Kim, S. Kim, B. H. Kang, K. H. Kim, G. T. Kim, Photoresponse of sol-gel-synthesized ZnO nanorods. Appl. Phys. Lett. **84**, 5022 (2004).

- [51] Y. Tao, M. Fu, A. Zhao, D. He, Y. Wang. *Journal of Alloys and Compounds* **489**,(1) 99 (2010).
- [52] M. Guo, P. Diao, S. Cai. *Journal of Solid State Chemistry* **178**,(6) 1864-1873 (2005).
- [53] T. Ma, M. Guo, M. Zhang, Y. Zhang, X. Wang. *Nanotechnology* **18**,(3) 0356051 (2007).
- [54] Q. Li, V. Kumar, Y. Li, H. Zhang, T.J. Marks, R.P. Chang. *Chemical Mater* **17**,(5) 1001-1006 (2005).
- [55] X. Y. Kong, Z. L. Wang, *Appl. Phys. Lett.* **84**, 975 (2004).
- [56] W. Peng, S. Qu, G. Cong, Z. Wang. *Crystal Growth & Design* **6**(6), 1518 (2006).
- [57] C. Pacholski, A. Kornowski, H. Weller. *Angewandte Chemie International Edition* **41**(7), 1188 (2002).
- [58] S. Xu, C. S. Lao, B. Weintraub and Z. N. Wang, Density-controlled growth of aligned ZnO nanowires arrays by seedless chemical approach on smooth surfaces. *J Mater Res*, **23**(8), 2072 (2008)
- [59] C. K. Xu, P. Shin, L. L. Cao, D. Gao. Preferential growth of long ZnO nanowire array and its application in dye-sensitized solar cells. *J PhysChem C*, **114**(1), 125 (2010).
- [60] C. H. Hsu, D. H. Chen, *J Nanotechnology* **21**, 285603 (2010).

Chapter No: 2**Characterization Techniques**

This chapter describes the background theories, principles and instrumental details of different characterization techniques namely X-ray diffraction (XRD), UV/Visible spectrometer, Scanning electron microscope (SEM) and Energy dispersive x-ray spectroscopy (EDX) which have been used to analyze and examine the properties of synthesized Al-doped ZnO nanorods samples.

2.1 X-Ray diffraction (XRD)

X-ray diffraction is a popular, non-destructive and powerful analytical technique used for materials characterization i.e. for structural elucidation and chemical composition. It also gives information about the physical properties of the materials because the physical properties of solid depend on the arrangement of atoms within the material [1]. Crystalline and non-crystalline (amorphous) materials can be differentiated through this reliable technique. This experimental technique has four basic features containing production of x-rays, diffraction of x-rays, detection of reflected x-rays and finally interpretation. By using this technique the chemical compound can be found out on the basis of their crystalline structure [2]. XRD is the finger print of crystalline materials. X-rays diffraction pattern could be obtained if the d spacing is comparable to the wavelength of the incoming X-rays and the structure of the material would be proper geometrical [3]. The structure of the sample can be identified by comparing the XRD pattern of the sample with the internationally recognized known standards in the JCPDS file. The XRD pattern of each material will always be unique and will never match with the pattern of any other material [4].

X-rays diffraction pattern provide the subsequent important information about the material.

- Detection of various phases present in the sample material.
- Evaluate configuration or atomic arrangement of a particular material structure.
- Unit cell structure identification, miller indices (hkl), lattice parameters.
- Separate crystalline materials from amorphous.
- Average crystalline size estimation can be made from the peak width.
- Orientation of a single crystal or grain.

To understand the X-rays diffraction phenomenon the fundamental knowledge about X-rays is needed to be understood.

2.1.1 X-rays

X-rays are electromagnetic radiations of wavelength 1 \AA smaller than the wavelength of visible light. X-rays are either generated by the inner shell transition of electrons (characteristic X-rays) in the atom or by the deceleration of high energy electron (continuous x-rays), when pass near to the nucleus. Besides XRD, X-rays are utilized in X-Ray Fluorescence (XRF) and in the most advanced instrument X-ray photoelectron spectroscopy (XPS) for the analysis of fluorescence, scattering, oxidation states, elemental composition and deposited film thickness of the sample material [5].

2.1.2 Bragg's Law

This law was first offered by William Lawrence Bragg in 1912 so called Bragg's law. The main purpose and extensive use of this law is to explain in detail the reflection of x-rays from the crystal planes. According to this law crystal planes act like a mirror which reflects the incident X-rays. When monochromatic beam of X-rays are allowed to hit the crystal surface of the sample, if the path difference of emerging reflected rays equal to the integral multiple of x-rays wavelength (λ) then Bragg's law will be fulfilled and diffraction will be occurred [6-7]. Thus, diffraction can occur only in case of constructive interference of reflected rays, while peaks of crystal planes are observed in the resulted XRD pattern. The figure 2.1 shows the Bragg's law from parallel planes of atoms.

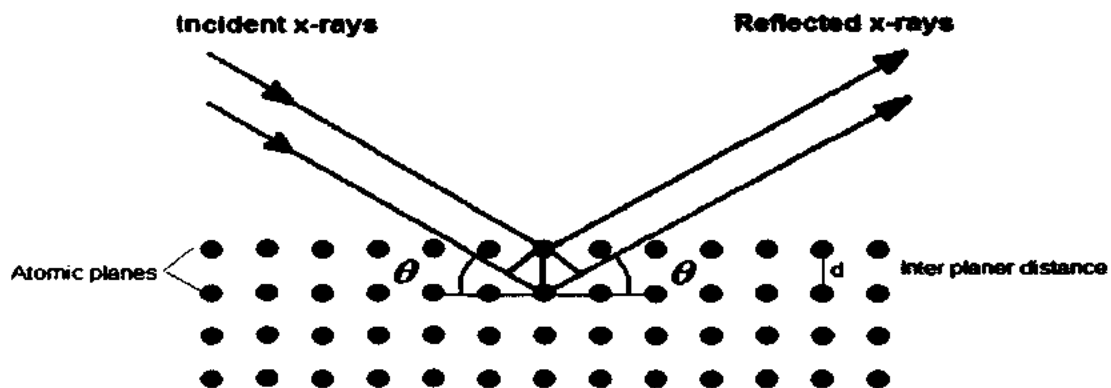


Figure 2.1: Graphical representation of Bragg's law [6].

The fundamental mathematical equation for diffraction is given below;

$$n\lambda = 2d\sin\theta \quad (2.1)$$

Where

n = integer

λ = X-rays wavelength

d = distance between atomic layers

θ = Bragg's angle

2.1.3 Crystal size determination

X-rays diffraction further used to calculate the grain size of the material. But it needs a bit careful analytical skills. First the full width at half maximum intensity of XRD peak as a function of Bragg's angle is examined [7-8]. Then by using D. Scherrer formula the crystallite size D can be estimated as

$$D = \frac{k\lambda}{\beta \cos\theta} \quad (2.2)$$

Where the extent λ is the x-ray wavelength, β is FWHM, θ is peak angle, constant $k = 0.9$.

The peak intensity in the spectrum demonstrates the concentration of the elements [9].

2.2 UV/Visible spectroscopy

UV-Visible spectroscopy is routinely carried out to study the optical properties of the material. It occupies light in the UV-visible region. Sometimes it is also known as absorbance or reflectance spectroscopy. It can be used for the quantitative determination of transition metal ions solutions and a high degree conjugated organic compounds [10]. This spectroscopy is very helpful to measure the transmission, absorption and reflection of pigments and filter like materials. Energy band gap of a material can easily be calculated from the reflectance and absorbance spectrum by using this technique. The scanning range for this kind of spectrometer is 190-900nm wavelength. The instrumental set up is shown in the figure 2.2.

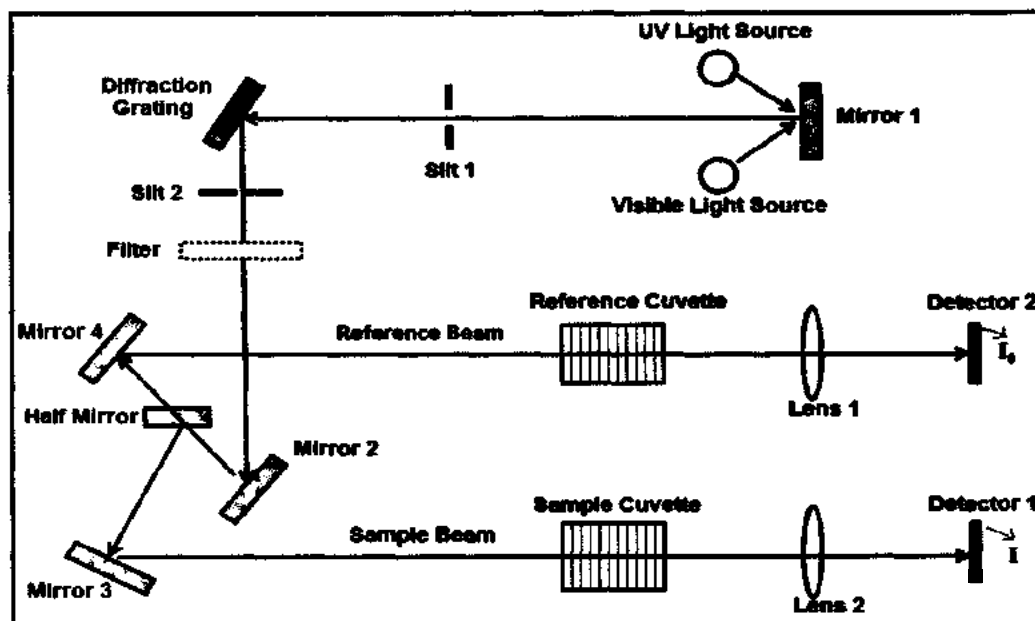


Figure 2.2: Experimental arrangement for UV-Visible spectrometer [11].

2.2.1 Working principle of UV/Visible spectrometer

The working principle of UV-visible spectrometer is very simple. It uses two light sources UV and visible. It consists of the following parts.

- Source of light (UV and Visible)
- Sample container
- Wavelength selector
- Detector
- Signal processor

The beam of light comes from both the sources and strikes the first mirror and moves towards the diffraction grating. The role of diffraction grating is to divide the light beam into its components. Each component of incident beam further splits into two beams with the help of half mirror. The first beam referred as sample beam passes through sample cuvette while the second beam which passes through reference cuvette is called reference beam. The intensities of both the beams are measured by the detectors. Then, the intensity of reference beams (I_0) and sample beam (I) are compared which give the resultant spectra on the computer screen.

2.3 Scanning electron microscope (SEM)

Scanning electron microscope is a versatile imaging technique mostly used for the surface morphology of the material. It is one of the most excellent and nondestructive characterization techniques which provide information about the grain size, particles distribution, orientation, structure and surface analysis of the material.

SEM operation is similar to Scanning Confocal Microscope (SCM) because in both cases the material is investigated by scanning the surface of the specimen [12, 13]. The only difference is that of source i.e. SEM uses electron beam while SCM uses light beam. Its resolution is higher compared to SCM, give 3D image with greater depth of field, that's why this technique is best to use for the characterization of nanomaterials. Figure 2.3 shows the block diagram of the various parts of SEM.

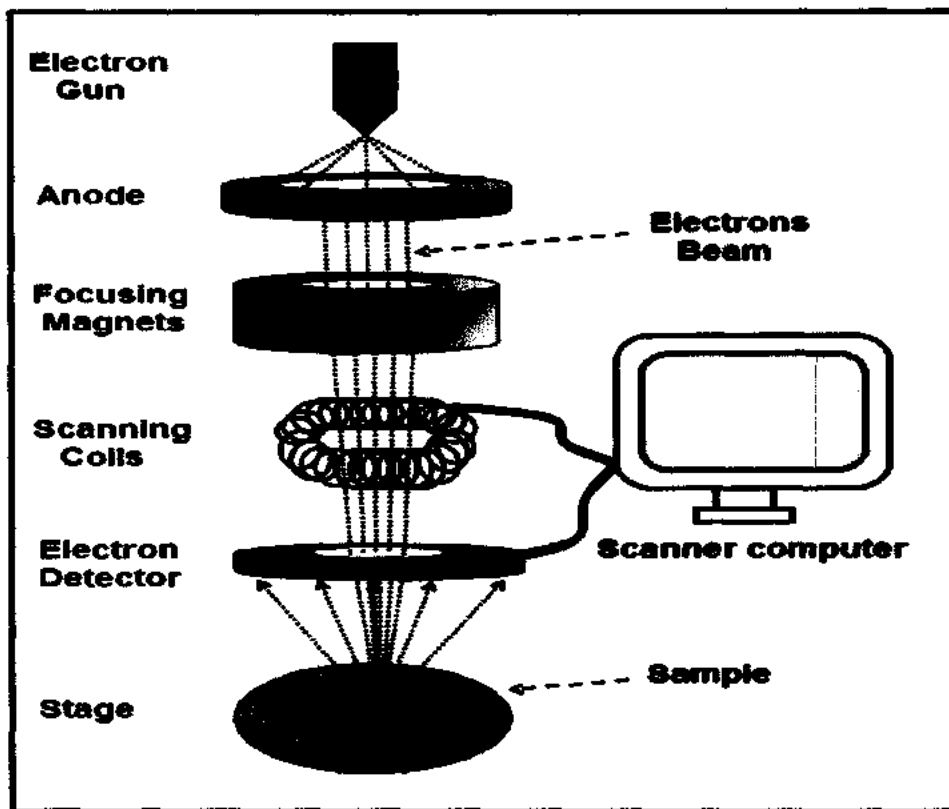


Figure 2.3: Scanning Electron Microscope construction [14].

The assembly of SEM consists of electron gun, Anode, series of electromagnetic lenses and signals detector. The electrons are emitted from electron gun and accelerated towards anode.

The high energy electrons beam usually ranging from few hundred eV to 100keV is focused near a size of about 1 to 5nm with the help of lenses setup. This narrow beam of electron strike the sample and a large number of interactions take place due to which electrons and photons are emitted from the surface of the sample [15-16]. It is essential to know about the detecting signals during the interactions of incident electrons and sample surface. Three major types of signals i.e. backscattered electrons, Secondary electrons and elemental X-rays are detected. The backscattered electrons and secondary electrons are produced due to the elastic and inelastic scattering of incident electrons with the sample atoms respectively. The ejection of core electron from the sample's atom results a characteristics X-rays photon or an Auger electron. All these signals are collected by the detector and further use them for the image formation of the sample. The magnification of SEM can be changed very easily by changing the scan area of the sample [17].

The resolution power of an instrument is

$$R = \frac{\lambda}{2N_A} \quad (2.3)$$

Where N_A is numerical aperture and λ is De-Broglie wavelength of an electron beam. The resolution of SEM is few nanometers and its magnification is almost 10 to over 300,000 [18].

2.4 Energy dispersive spectroscopy (EDX)

EDX is an analytical tool employed to study the composition of elements in the specimen. It is also called Energy Dispersive spectroscopy (EDS). Usually its operational working is attached to SEM. EDX consists of four basic components which are

- Electron source
- X-rays detector
- Pulse processing
- Analyzer

To analyze the elemental composition of the sample material through EDX process, high energy beam of electrons is bombarded on the sample which interacts with the inner shell electrons of the sample's atoms. Due to extra high enough energy, they eject electrons

from the inner shells of the sample's atom. In this way a vacancy of electron is created in the inner shell of sample's atom [13]. Next, to fill this vacancy an electron transition takes place. The higher shell electron jumps and fills the created vacancy. During the transition a photon of energy $h\nu$ is emitted from the atom as shown in the figure 2.4. In this way a large number of photons are emitted from the atoms of the specimen. These series of photons have unique characteristics (frequency, wavelength), does not match with any other atoms. That's why they are called characteristic x-rays. This is the reason that they are used for the identification of elements. The peaks in EDX spectra correspond to energy levels give information about the elements present in the sample material.

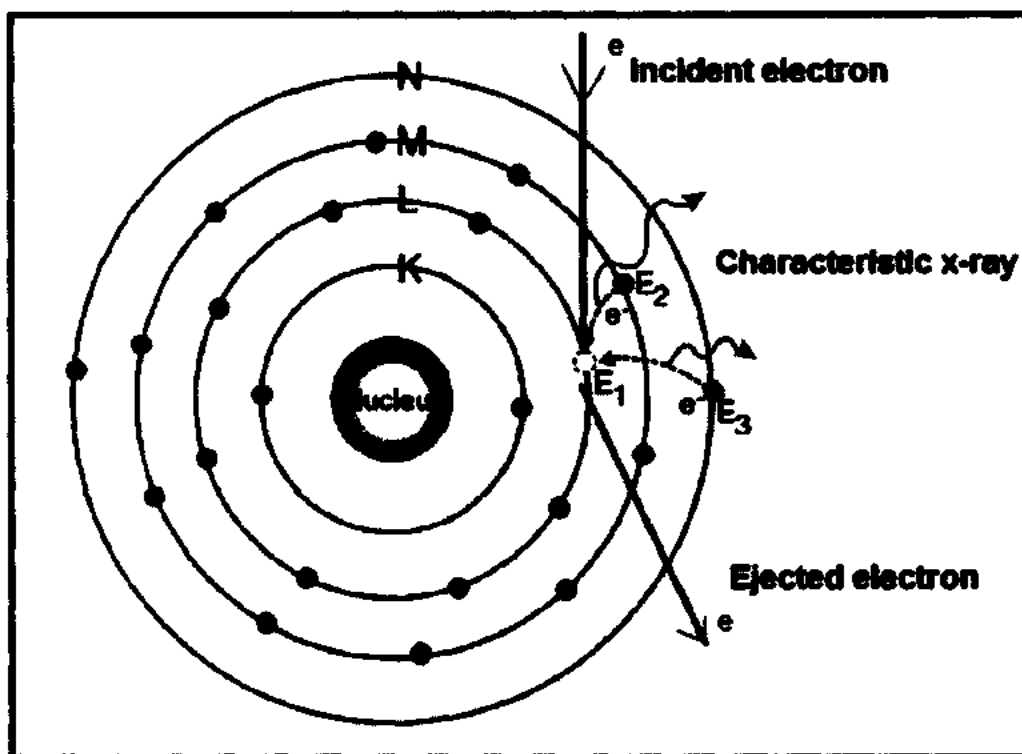


Figure 2.4: Working principle of EDX [19].

References

- [1] R. S. Mishra, C. E. Lesher, and A. K. Mukherjee, *J. Amer. Ceramic. Society.* **79**,2989 (1996).
- [2] G. D. Zhan, J. Wan, J. Garay, and A. K. Mukherjee, *Scriptamaterialia.* **24**, 7737 (2000).
- [3] K. N. Lewis, M. V. Thomas, D. A. Puleo, *J. Mat. Sci.* **17**, 531 (2006).
- [4] L. Hollaway, *Handbook of Polymer Compites for Engineering*, WoodheadPublishing, (1994).
- [5] H. P. Klug, L. E. Alexander, *X-ray Diffraction Procedures for Polycrystalline and Amorphous Materials*, John Wiley New York, (1974).
- [6] A. R. West, *Basic Solid State Chemistry*, 2nd Edition, John Wiley and Sons Publishers, (1995).
- [7] B. D. Cullity, S. R. Stock, *Elements of X-ray Diffraction*, 3rd Edition, Addison-Wesley Publisher, (2001).
- [8] L. H. Schwartz, J. B. Cohen, *Diffraction from Materials*, 2nd Edition, Addison-Wesley Publisher, (1987).
- [9] B. Clafin, D. Look, S. Park, G.Cantwell, Persistent n-type photoconductivity in p-type ZnO. *Journal of Crystal Growth*, **287(1)**, 16 (2006).
- [10] Skoog, *Principles of instrumental Analysis*, 5th Edition, Thomson Books/Cole Publisher, (2007).
- [11] K. Wasa, *Thin Film Technology and Applications*, 1st Edition, North-Holland Publisher, (1985).
- [12] D. McMullan, *J. Proc Roy Micro Society.* **23**, 283 (1988).
- [13] G. Goldstein, I. Newbury, D. E. Echlin, P. Joy, D. C. Fiori, C. Lifshin, *Scanning Electron Microscopy and X-ray microanalysis*, 2nd Edition, Plenum Press Publisher, (1981).
- [14] W. Clegg, *Crystal Structure Determination*, Oxford University Press, (1998).

- [15] T. Everhart, E. Thornley, *J. Scientific Instrument.* **37**, 246 (1960).
- [16] D. Attwood, *Soft X-rays and Extreme Ultraviolet Radiation*, Cambridge University Press (1999).
- [17] S. Wischnitzer, *Introduction to Electron Microscopy*, Pergamon Press, (1981).
- [18] M. Von Ardenne, *Improvement in electron Microscopes*. 1stEdition, Plenum PressPublisher, (1937)
- [19] J. I. Goldstein, H. Yakowitz, *Practical Scanning Electron Microscopy*, Plenum Press, (1977).

Chapter No:3**Experimental and Synthesis**

To synthesis ZnO nanorods a number of methods have been used by the researchers. Some of the most common methods are introduced here.

3.1 Pulsed laser deposition method

The PLD technique is based on light matter interaction. In this method a stream of high power laser pulses focused onto a target material with the help of optical lenses. When the interaction between laser beam and target material take place, highly energetic ionized species are generated inside a vacuum chamber. The ionized species also called plasma plume. Before starting the deposition on the desired substrate, species are dissociated from the target material in order to expand plume from the target [1-2]. Next, the ablated species (atoms and ions) will tend to move in the direction of the target, hit the substrate surface and will condense on it. In this way deposition start and growth take place on the substrate. The deposition depends upon the system parameters (Laser beam intensity, substrate temperature, pulse duration, oxygen pressure, separation between target material and deposition substrate). For high quality ZnO nanorods growth these parameters must be adjusted [3].

3.2 Chemical vapor deposition

Initially CVD method was considered semiconductor thin film process but now it has been applied for 1D ZnO nanorods growth. This method is very interesting not only for high quality 1D nanorods growth but also valid for large scale production. Several adaptations have been made in this method depending on the precursors. By using metal-organic precursors, the method is known as metal-organic chemical vapor deposition (MOCVD) [4]. If hydride or halide precursors are used then its name is altered to hydride or halide CVD or HCVD [5-6]. In this method vapor-phase precursors containing the required chemical elements are delivered into the growth region by carrier gas. ZnO nanorods growth occurs as a result of chemical reactions on the surface of the substrate.

ZnO quantum dots and thin film have already been reported in the research by using MOCVD [7]. Its development in the formation of ZnO nanorods and nanoneedles is very recent. Applying this technique, Yi et al. [8] obtained aligned arrays of ZnO nanorods and nanoneedles.

One of the most important advantages of catalyst-free MOCVD is the easy fabrication of highly pure nanorods of ZnO [9].

3.3 Magnetron sputtering method

Sputtering is one of the popular, simple compared to CVD and a versatile growth technique for ZnO nanostructure. It is sometimes named as RF magnetron and DC magnetron sputtering depending on the energy source. Usually two types of energy sources are used i.e. direct current (DC) for conducting target and radio frequency (RF) for non-conducting target. If the energy source is direct current (DC) then it is called DC sputtering if the source is radio frequency (RF) then it is called RF magnetron sputtering. The purpose of the energy source is to maintain the plasma gaseous state. In the beginning it was preferable method because of avoiding high temperature and reasonable quality film [10-11]. The configuration is that, the target is eroded, neutral particles are emitted from the target with the bombardment of argon ions, they travel in a straight path and deposited on the surface of the substrate if placed in the path of emitted particles. The crystal size may change with the deposition angle [12]. The growth of ZnO usually carried out in the presence of Argon and Oxygen mixture. The Argon gas influences the sputtering while oxygen gas (O_2) serves as reactive gas. By using sputtering technique the quality and structure of growth and deposition can be improved to some extent with working distance, Oxygen partial pressure, Pressure inside the tube, target material, Gaseous plasma.

3.4 Vapour phase technique

1D nanostructure ZnO can be synthesized by vapour phase technique. It is based on the principle of thermal evaporation. The vapour phase evaporation method is a simple process in which vapour species are first generated from condensed or powder source material are evaporated, these vapour species are subsequently react and condensed onto the surface of the desired solid substrate under certain condition of pressure and temperature. Usually the substrate is lying in the lower temperature zone than that of source powder. The temperatures of the source will always be less than the melting point of the source to avoid the source material from melting. This may be the most widely explored approach to the formation of ZnO nanorods because it can easily be carried out in a simple horizontal tube both ends preserved by rubber O-rings [13]. Although the exact and proper mechanism of this method for one dimensional nanorods growth is still not clear but many researchers have been synthesis ZnO nanorods by

using this technique. For example, using vapour phase process, Zhang et al [14] and Kong et al [15] have fabricated ZnO nanorods and nanowires by simply evaporating powder of ZnO. Lao et al [16] and Wang et al [17] synthesized hierarchical and nanoribbon of ZnO using this concept respectively. Considerable change can occur in the morphology of the resultant nanostructure by changing the composition of the source material [18].

All these methods have complicated procedures and precautions controlling synthesis background, but the Chemical bath deposition (CBD) method is prestigious, low cost and rapid synthesis method. So this method is preferable over all others method.

3.5 Chemical bath deposition method

In the 20th century CBD method was obviously recognized as an important and significant technology for material fabrication and mostly for single crystal growth [19]. This method was first time reported by Andres Verges et al. [20] in 1990. More than 10 years later, another research group Vayssieres et al. [21] also used this simple technique for ZnO nanorods growth on the surface of conducting glass. Particularly, in the last years this method was developed, exploit and utilize to obtained nanomaterials of different structure. For example, nanorods, nanotubes, thin film nanowires etc. The quality and morphology of ZnO nanorods can be controlled with different parameters which have already been discussed in first chapter.

Aqueous growth solution of Zinc nitrate or Zinc acetate is prepared by using magnetic stirrer. Then the substrate is suspended in the solution with some support like Teflon rod and covered it. In the next step the substrate suspended solution is placed in a temperature zone (oven). Generally, Zinc nitrate or Zinc acetate source of Zn^{+2} ions and Hexamethyltetramine (HMTA) or Ammonia (NH_3) source of OH^- ions are used in this technique to grow ZnO nanorods. In this research work Al-doped ZnO nanorods have been grown on the surface of substrate by using this method.

3.5.1 Advantages of CBD method

- i. CBD method is a simple and comprehensible technique.
- ii. It is economical to a great extent because of low cost of instrumentation and precursors.
- iii. By using this effortless technique uniformity of nucleation, orientation, diameter, and length of nanorods can easily be controlled.

- iv. Variety of nanostructure can be prepared by hydrothermal method for example Powder, fiber, coating on metal and glass, polymers etc.
- v. Almost the processes discussed before this method require high temperature and high pressure but in CBD method these conditions are usually passed up.
- vi. Due to the fact of low reaction temperature i.e. close to the living conditions, it is considered an environmentally friendly procedure and avoids the volatilization problems.
- vii. A large amount of energy is needed to create vapor or plasma plume within a chamber. A very less amount of energy consumption is needed in the formation of growth solution. Also the time consuming is minor because no milling and mixing steps are involved [22].

3.6 Experimental

3.6.1 Materials used

For seed layer Zinc acetate hexahydrate, 2- Methoxyethanol and Monoethanolamine were purchased from Sigma Aldrich and used as received. Commercially available microscope glass slides were used as substrates. For ZnO and Al-doped ZnO nanorods growth, Zinc Acetate hexahydrate and aqueous ammonia solution (33 wt. %) and aluminum nitrate nonahydrate were also purchased from Aldrich. Distilled water is used as a solvent.

3.6.2 Substrate cleaning

Before growth, substrate cleaning is essential to make it dirt free, and remove any other organic residual. First of all the glass slides were cut carefully with the help of diamond cutter of size (0.5inX0.5in). Ahead of deposition, these substrates were nicely cleaned in acetone by ultrasonification for 30 minutes at 50 °C. The same process is frequent for ethanol and distilled water. Then the cleaned substrates were dried in oven at 90 °C for 20 minutes. The steps are shown in figurefigure 3.1.

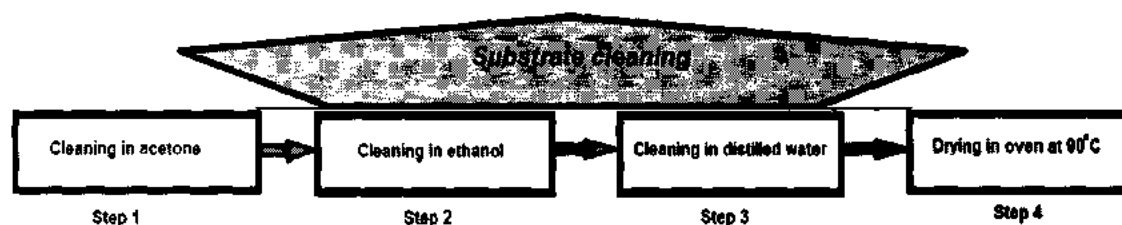


Figure 3.1: Substrates cleaning steps

3.6.3 Seed Solution

The sol solution of (0.4 M) for ZnO seed was prepared by dissolving 2.4 gm zinc acetate hexahydrate in 20ml 2-methoxyethanol. For 0.5h it was sonicate at 50 °C for the purpose of mixing and dispersion. To make the solution clear and homogenous it was stirred for 1h. Monoethanolamine of 0.5ml was added to the solution for stabilization under continues stirring [23]. With the addition of Monoethanolamine, the solution becomes transparent. Stirred it again for 1h and finally got transparent sol solution for seed layer.

3.6.4 Preparation of ZnO seed by Spin coating

The role of seed layer cannot be ignored in nanorods growth. The solution was spin coated on the cleaned glass substrates. The substrate was stick with the help of double sided tapat the stage of sample and the spin coater was set to rotate at 3000rpm for 30 seconds, to optimize uniform seed layer. Prior to run the spin coater 4 to 5 drops are put on the center of the substrates with the help of dropper in order to wet its upper surface completely. The purpose of completely wetting is to obtain uniformity in the nanoparticles of seed. After that, the coated substrates were pre-heated at 350°C in a furnace for 20 minutes to evaporate the solvent and remove organic residues materials. Next, the seeded substrates were cooled in a furnace to avoid the cracks. Finally, the seed coated substrates were annealed in a furnace at 500°C for 2 h, because the annealing of seed layer has substantial effect on nanorods arrays to be grown over it [33-34]. For several times coating the process is repeated. In this way a series of seed coated substrates were prepared to study the effect of seed on the surface morphology of nanorods to be grown over it.

3.6.5 Synthesis of Al-doped ZnO nanorods

To grow vertically well aligned Al-doped ZnO nanorods and to study and investigate the effect of seed and dopant concentration on the morphology and properties of ZnO nanorods, a series of experiment was performed. Also for this purpose a varieties of solutions were prepared with different combinations of precursor (Zn) and dopant (Al) in the present work.

For 0.5wt.% Al-doped ZnO nanorods, 0.1 molar (0.1 M) solution of zinc acetate hexahydrate was prepared by dissolving 2.181gm zinc acetate in 100 ml distilled water with continues stirring for 2 hrs. The color of the solution was milky white. Now aluminum nitrate nonahydrate of amount 0.0188gm was added to the solution as a dopant. With the addition of aluminum nitrate, color of the solution changed from milky white to transparent. A complexing agent ammonium hydroxide (33% NH₃ in water) of 5ml was added drop wise to the solution

under vigorous stirring to set the pH at 11. The resulting solution was stirred more for 1 h and covered it with aluminum foil to stop the evaporation and maintain the pH. With the addition of NH_3 the color of the solution again changed to milky white.

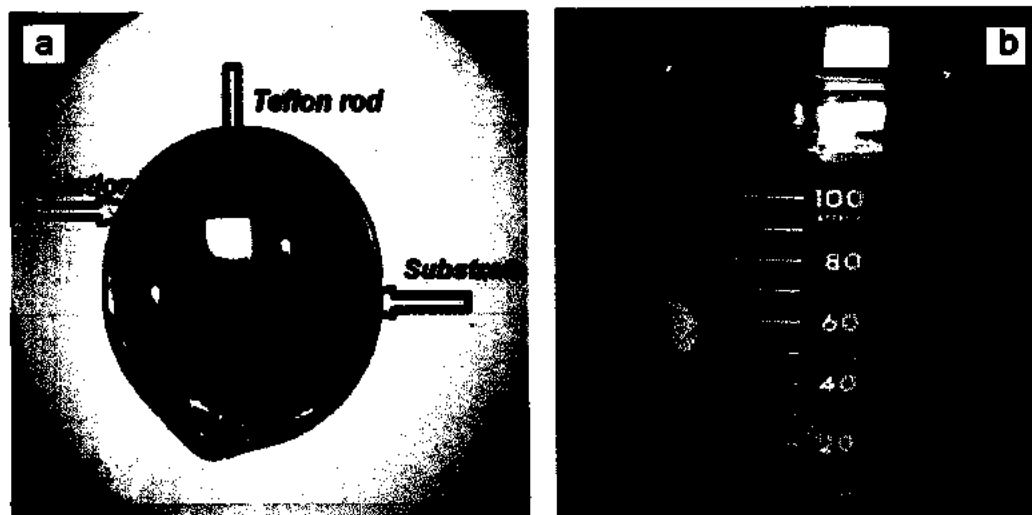


Figure 3.2: Al-doped ZnO solution (a) Top view (b) Side view.

Now to prepare a series of samples, solutions of different concentration are formulated by using the same procedure as that for 0.5 wt.% Al doping. The series of samples is given in the Table 3.1.

Table 3.1: A series of samples with different precursor concentration ratios.

Sample	Amount of $\text{Zn}(\text{CH}_3\text{OO})_2 \cdot 6\text{H}_2\text{O}$ (g/mol) for 0.1M solution	Amount of $\text{Al}(\text{NO}_3)_3 \cdot 9\text{H}_2\text{O}$ (g/mol) for 100ml solution
Undoped	2.195mg	0.0000mg
0.5 wt.%	2.181mg	0.0188mg
1.0 wt.%	2.173mg	0.0375mg
2.0 wt.%	2.151mg	0.0750mg
4.0 wt.%	2.107mg	0.1500mg

Next, the ZnO seed coated glass substrates were submerged into the synthesized solutions of 100ml having different concentration of Al. The substrates were suspended in Teflon rods in

such a way that the seed coated surfaces were face down in the growth solution. After that, took an observation from the side of the beaker to ensure that the suspended substrates within the solutions are in horizontal level. Now the beakers are covered properly with aluminum foil to minimize the evaporation and to sustain the pH at 11. Next, the beakers were placed in a pre-heated oven at 90°C for 6 hrs. After 6hrs, the substrates were taken out from the beakers and rinsed several times with distilled water. After drying at room temperature, finally they were annealed at 300 °C for 1 h in a hot furnace. For comparison study, Al-doped ZnO nanorods were also grown directly on seedless substrates. To summarize the whole work a flow chart is shown in the figure 3.3.

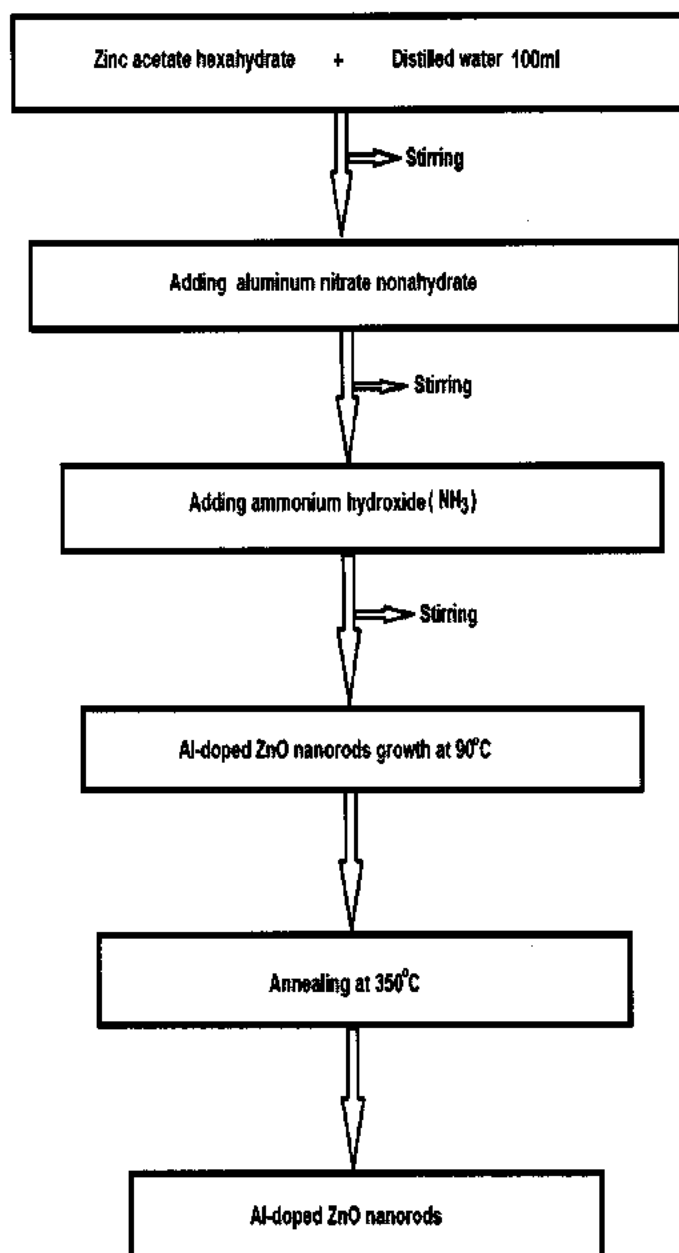


Figure 3.3: Flow chart for Al-doped ZnO nanorods preparation.

References

- [1] T. Premkumar, Y. S. Zhou, Y. F. Lu, Optical and field-emission properties of ZnO nanostructures deposited using high-pressure pulsed laser deposition. *J Appl Mater Interfaces*, **2(10)**, (2010).
- [2] J. H. Choi, H. Tabata, T. Kawai, *J. Cryst. Growth*, **226** (2001).
- [3] J. Schou, Physical aspects of the pulsed laser deposition technique, the stoichiometric transfer of material from target to film. *Applied Surface Science*, **255(10)**, 5191 (2009).
- [4] Y. Liu, C. R. Gorla, S. Liang, N. Emanetoglu, Y. Lu, H. Shen, M. Wraback, *Journal of Electronic Materials*, **29**, 69 (2000).
- [5] M. Kasuga, S. Ogawa, *Japanese Journal of Applied Physics*, **22**, 794 (1983).
- [6] N. Takahashi, K. Kaiya, T. Nakamura, Y. Momose, H. Yamamoto, *Japanese Journal of Applied Physics*, **38**, 454 (1999).
- [7] F. Heinrichsdorff, M. H. Mao, N. Kirstaedter, A. Krost, D. Bimberg, A. O. Kosogov, P. Werner, Room-temperature continuous-wave lasing from stacked InAs/GaAs quantum dots grown by metalorganic chemical vapor deposition *Appl. Phys. Lett.* **71**, 22 (1997).
- [8] W. I. Park, D. H. Kim, S. W. Jung, G. C. Yi, Metalorganic vapor-phase epitaxial growth of vertically well-aligned ZnO nanorods *Appl. Phys. Lett.* **80**, 4232 (2002).
- [9] W. I. Park, G. C. Yi, M. Y. Kim, S. J. Pennycook, ZnO nanoneedles grown vertically on Si substrates by non-catalytic vapor-phase epitaxy *Adv. Mater.* **14**, 1841 (2002).
- [10] P.J. Kelly, R.D. Arnell. *Vacuum* **56**, 159 (2000).
- [11] J. L. Vossen, *Physics of Thin Films*, Academic Press, New York, **9**, 1 (1977).
- [12] S. Mukhtar, A. Asadov, W. Gao. *Thin Solid Films* **520(9)**, 3453 (2012).
- [13] R. S. Wagner, *Whisker Technology* ed A P Levitt (New York: Wiley-Interscience), **47** (1970).
- [14] Y. Zhang, N. Wang, S. Gao, R. He, S. Miao, J. Liu, J. Zhu, X. Zhang, A simple method to synthesize nanowires *Chem. Mater.* **14**, 3564 (2002).
- [15] Y. C. Kong, D. P. Yu, B. Zhang, W. Fang, S. Q. Feng, Ultraviolet-emitting ZnO nanowires synthesized by a physical vapor deposition approach *Appl. Phys. Lett.* **78**, 407 (2001).
- [16] J. Y. Lao, J. G. Wen, Z. F. Ren, Hierarchical ZnO nanostructures *Nano Lett.* **2**, 1287 (2002).

- [17] Wang, Z. Lin, Zinc oxide nanostructures growth, properties and applications." *Journal of Physics, Condensed Matter* **16(25)**, 829 (2004).
- [18] P. X. Gao P X, Z. L. Wang, *J. Phys. Chem. B* **106** 12653 (2002).
- [19] R. E. Riman, *Ann. Chim. Sci. Mat.*, **27(6)**, 15 (2002).
- [20] M. A. Verges, A. Mifsud M, C. J. Sema, *J. Chem. Soc, Faraday Trans*,**86**, 959 (1990).
- [21] L. Vayssieres, C. Sathe, S.M. Butorin, D. K. Shuh, *J. Nordgren, J. Guoet*,*J. Phys. Chem. B* **105**, 3350 (2001).
- [22] M.Yoshimura,W.Suchanek, *Solid State Ionics*, **98**, 197 (1997).
- [23] S. Kim, H. Park, G. Nam, H. Yoon, B. Kim, I. Ji, Y. Kim, I. Kim, Y. Park, D. Kang, and J. Y. Leem, *Electron. Mater. Lett.*,**10(1)**, 81 (2014).

Chapter No: 4

Results and Discussion

This chapter presents the consequences of the synthesized samples. Different techniques like XRD, FESEM, XRD, EDS and UV-Visible Spectrophotometer were used which we have already discussed in the second chapter. With the help of these techniques we have inspected all the samples structurally, morphologically, compositionally and optically as discussed in detail.

4.1 XRD results

XRD analysis was conducted for structural investigation of ZnO nanorods and Al-doped ZnO nanorods with different doping concentration grown on ZnO seed coated glass substrates. As from the combined XRD pattern of undoped and Al-doped ZnO nanorods grown on seeded glass substrates shown in the figure 4.1. As expected, we can observe that the peak for (002) plane at an angle of 34.54° is stronger and leading over all other peaks of (100), (101) and (102) planes at an angles 31.87° , 36.38° and 47.65° respectively (reference card No. 01-079-0208). This high intense peak of (002) plane specifies and gives the proof of hexagonal wurtzite crystal structured ZnO. However, the high intense peak of (002) plane in all pattern further indicates that the grown nanorods are highly oriented in the c-axis direction. No diffraction peaks of Zn, Zn(OH)₂, metal aluminum, aluminum oxide or any other impurity phases are detected for 0.5 wt.%, 1 wt.%, 2 wt.% and 4 wt.% Al doping excluding ZnO [1-2]. It provides that Al doping does not affect significantly the crystal orientation of wurtzite type ZnO nanorods and their structure.

This analysis reveals that only single phase hexagonal wurtzite type structure of ZnO is present. Also it has been noticed from the XRD pattern that with Al doping the peaks are slightly shifts to a higher degree angle which might be appear due to the substitution of Al⁺³ into the Zn⁺² lattice sites having small ionic radii difference ($r_{Zn^{+2}} = 0.074\text{nm}$ and $r_{Al^{+3}} = 0.054\text{nm}$). Nevertheless, by increasing doping concentration of Al, the intensity of the (100) and (101) planes increases gradually. So it is believed that Al is successfully doped in ZnO lattice [3]. But at the same time the lower concentration of aluminum doping have significant effect on the crystal size and orientation of ZnO nanorods.

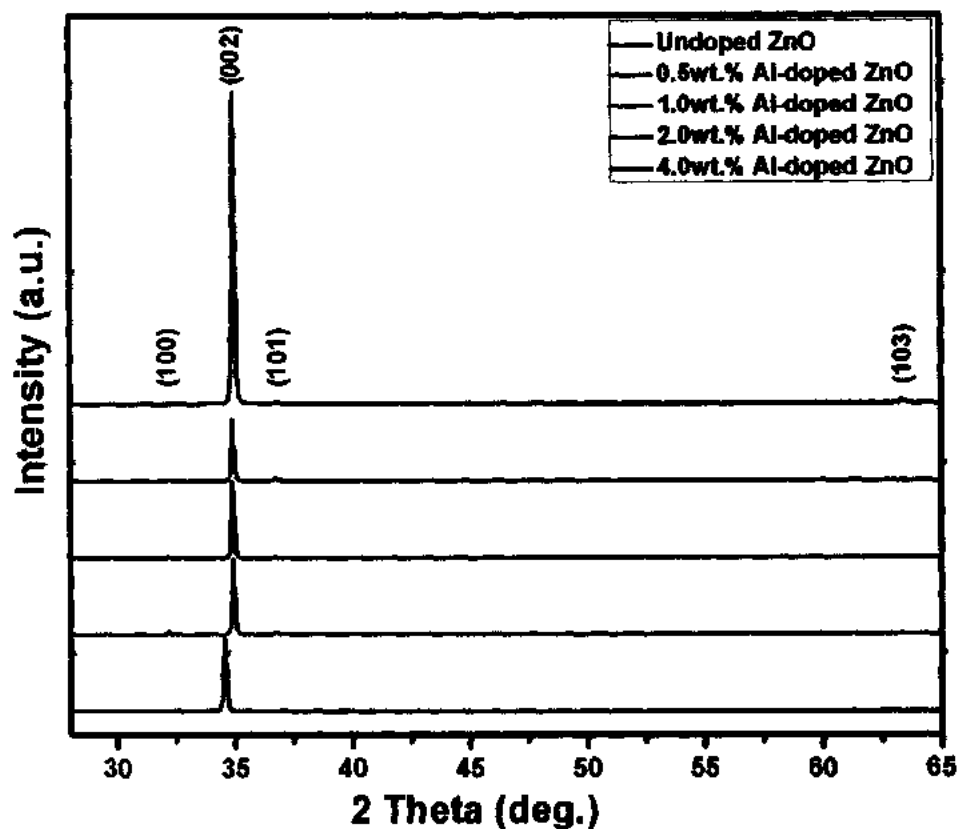


Figure 4.1: XRD patterns of Undoped, 0.5 wt.%, 1.0wt.%, 2.0 wt.% and 4.0 wt.% Al-doped ZnO nanorods.

The average crystallite size was calculated by using Debye Scherrer formula [4].

$$D = \frac{K\lambda}{B\cos\theta} \quad (4.1)$$

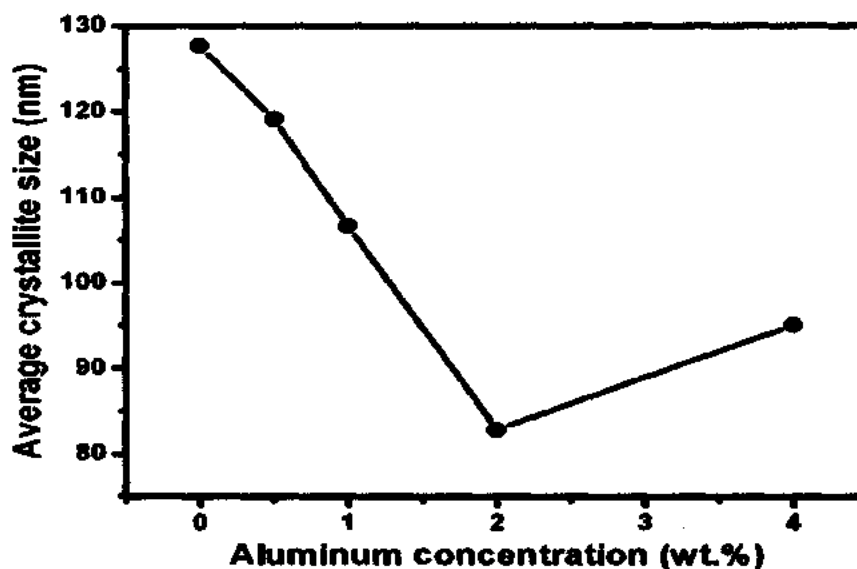
Where D is the crystallite size, $K = 0.9$ is constant, λ is the wavelength having value 1.54 \AA , B is the FWHM of the peak and θ is the peak position in XRD pattern.

The average crystallite size of ZnO and Al-doped ZnO with different concentration, for the three most prominent and high intense peaks are calculated as given in the table.

Table: 4.1. Average crystallite size of undoped and Al-doped ZnO nanorods.

Sample	Average crystallite size for three most prominent peaks (nm)
Undoped ZnO nanorods	127.73
0.5 wt.% Al-doped ZnO nanorods	119.14
1.0 wt.% Al-doped ZnO nanorods	106.44
2.0 wt.% Al-doped ZnO nanorods	82.87
4.0 wt.% Al-doped ZnO nanorods	95.10

It is observed that the average crystallite size of ZnO nanorods slightly decreases with the Al doping. It is believed that this may be due to the incorporation of Al into ZnO lattice and replacement of bigger Zn^{+2} ions by comparatively smaller Al^{+3} ions. As the radius of Al^{+3} ions is smaller compared to Zn^{+2} ions. It leads to a decrease in the lattice constant which in turn is responsible for the variation in the crystallite size. Figure 4.2 shows the variation in the average crystallite size of ZnO nanorods with different Al contents in a series, but the decrease occurred in the crystallite size is not in any regular pattern.

**Figure 4.2:** Average crystallite size variations with different Al concentrations.

4.2 Optical results

4.2.1 Energy Band gap

The optical behavior and an imperative parameter band gap of ZnO and Al doped ZnO nanorods was studied by means of diffused reflectance spectra (DRS). Since, it is known that ZnO is a direct band gap material. The band gap of the material from DRS can be determined by using KubelkaMunk equation as [5]

$$F(R_{\infty}) = \frac{(1-R_{\infty})^2}{2R_{\infty}} = \frac{K}{S} \quad (4.2)$$

Where

$F(R_{\infty})$ is remission or K M function,

R_{∞} is the diffused reflectance of the material i.e. $R_{\infty} = R_{\text{sample}} / R_{\text{standard}}$ [6].

K is the absorption coefficient and S is the scattering coefficient.

According to Tauc relation the absorption coefficient (α) and band gap (E_g) of semiconductor are related as [7]

$$\alpha h\nu = C (h\nu - E_g)^n \quad (4.3)$$

Where C is the constant of proportionality and $h\nu$ is the photon energy. The n value depends on the material, for direct band gap materials $n = \frac{1}{2}$ while for indirect band gap materials $n = 2$. Since our material ZnO is direct band gap semiconductor material. Thus the above equation can be written as

$$\alpha h\nu = C (h\nu - E_g)^{1/2} \quad (4.4)$$

When the material is illuminated at 60° incidence or another word the material scatters in perfectly diffuse manner, then in this case the K-M absorption coefficient will be double times of linear absorption coefficient i.e. $K=2\alpha$. In this case, in equation (1) The K-M scattering coefficient S is taken constant. From equation (1) and (2) we get the equation

$$[F(R_{\infty})h\nu]^2 = C_1(h\nu - E_g)^{1/2} \quad (4.4)$$

To extract the band gap energy value of the sample, first obtained $F(R_{\infty})$ from equation (1) then plot $[F(R_{\infty})h\nu]^2$ verses $h\nu$. The straight line drawn to the energy axis, which cut the

energy axis at $[F(R_{\infty}) h\nu]^2 = 0$ gives the value of the band gap of the material. As a result, to acquire the values of the optical band gap of ZnO, plotted $[F(R_{\infty}) h\nu]^2$ against $h\nu$ (photon energy). The band gap value of undoped ZnO nanorods is shown in the figure. 4.3. The undoped ZnO is taken as a reference for Al doped samples.

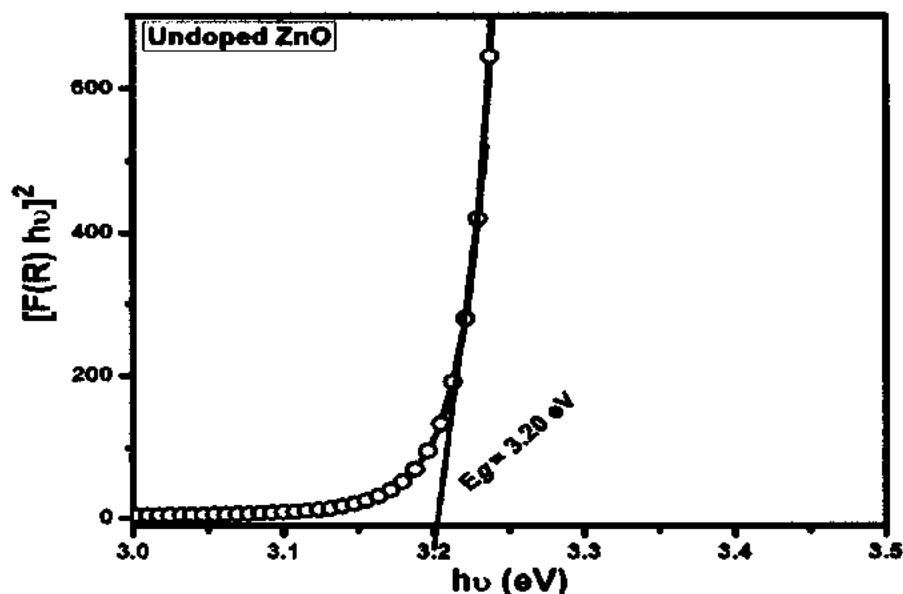


Figure 4.3: Energy band gap of undoped ZnO nanorods from DRS spectra.

Next the band gap of the series samples are calculated from K-M transferred reflectance spectra as illustrated in the figure 4.4. it is found that the band gap of ZnO enhances with aluminum doping and also the linearity illustrate that it is direct band gap material which is particularly suitable property for photovoltaic application. The increase in the band gap of ZnO with Aluminum doping might be explained in terms Burstein-Moss effect. According to this effect, with Al doping the electron carrier concentration in the host ZnO has been increased, which results in the form of shifting Fermi level to the conduction band and causes to wider the band gap. The wider energy band gap would possibly improve the transmission in the visible region. From the table 4.2, obviously the band gap of ZnO nanorods increases which is one of the evidence of successful doping. It was also noted that at higher level of doping the transmittance decreases which is due to the increase in disorder in the crystallinity.

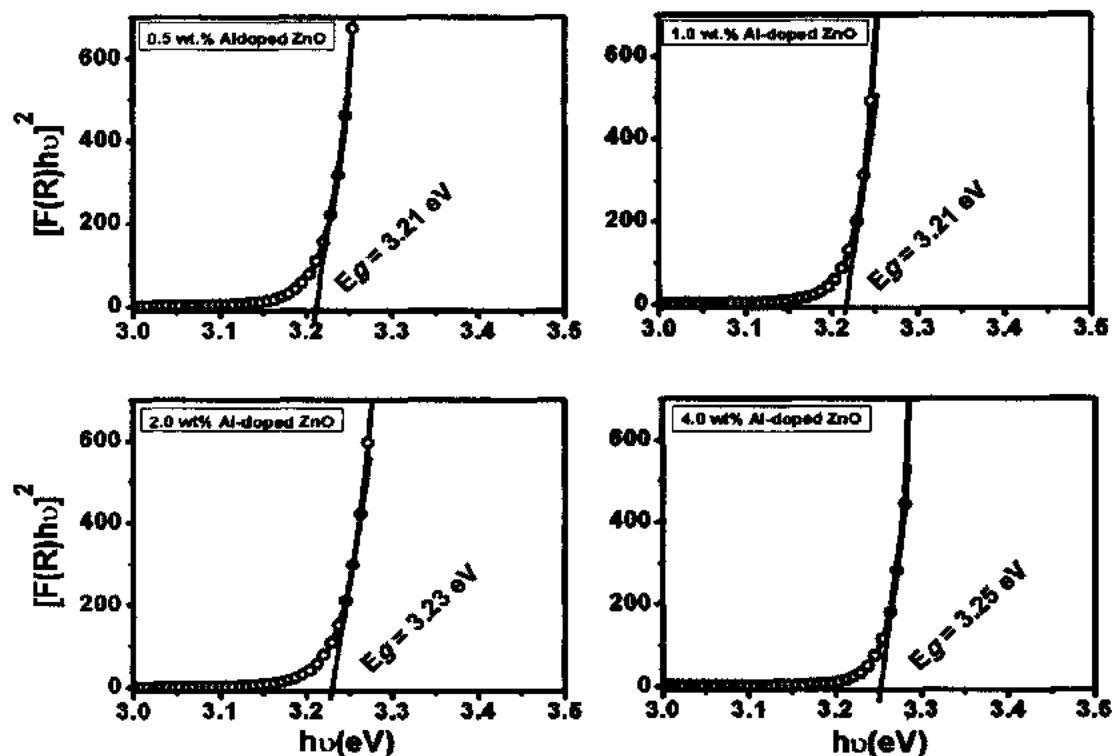


Figure 4.4: Plots of $[F(R_{\infty})hv]^2$ vs. hv shows K-M transferred reflectance spectra of 0.5wt.%, 1.0wt.%, 2.0wt.% and 4.0wt.% Al-doped ZnO nanorods.

Table: 4.2. Band gap values of undoped and Al-doped ZnO nanorods.

Sample	Band gap value (eV)
Undoped ZnO nanorods	3.20
0.5 wt.% Al-doped ZnO nanorods	3.20
1.0 wt.% Al-doped ZnO nanorods	3.21
2.0 wt.% Al-doped ZnO nanorods	3.23
4.0 wt.% Al-doped ZnO nanorods	3.25

4.2.2 Transmittance

Now to investigate the optical transmittance of ZnO nanorods and also to study the effect of Al doping on its transmittance UV-visible transmittance data was obtained in the wavelength range of 200-800nm. All the samples show high transmittance in the visible range of wavelength 400nm-800 nm as shown in the figure 4.5.

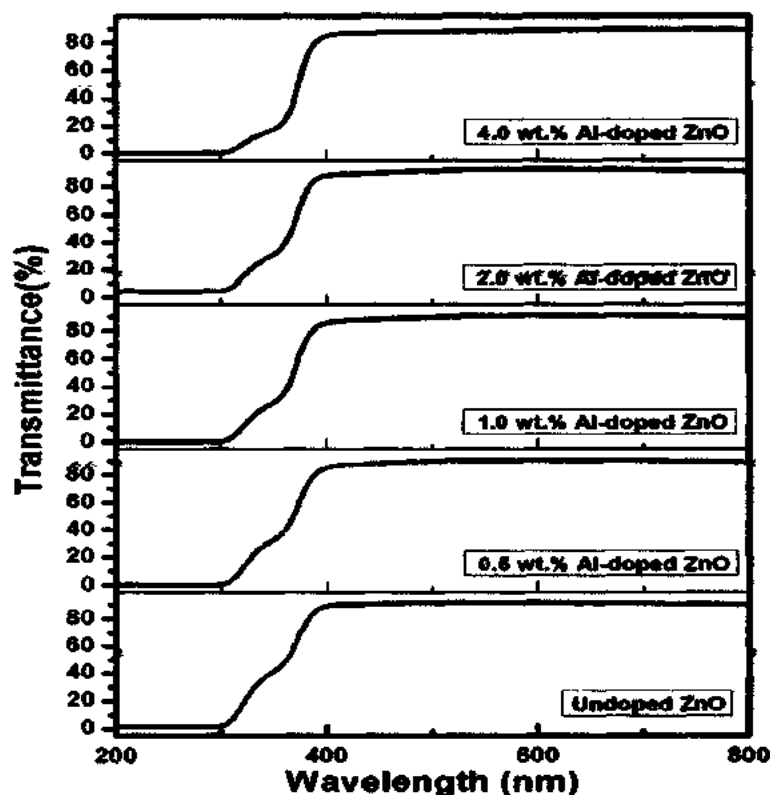


Figure 4.5: Transmittance spectra of Undoped and 0.5 wt.%, 1.0 wt.%, 2.0 wt.%, 4.0 wt.% Al-doped ZnO nanorods.

A smaller variation is observed in the transmittance of ZnO nanorods with Al doping. It was found that the transmittance of 2% Al-doped ZnO nanorods is almost 92% in the range of wavelength 500nm to 800nm as shown in the inset of figure 4.6. So, this result demonstrates that improvement has been occurred in the transmittance of ZnO nanorods with Al doping.

The reason for that may be that the 2 wt.% Al-doping nanorods provides more voids compared to 0.5 wt.%, 1.0 wt.% and 4.0 wt.% doped nanorods which results a decrease in the optical scattering and enhance the transmittance. The second possible evidence is that the dopant atoms Al provide free carriers which bring a small shift in the Fermi level and increases the energy band gap. This increase in the energy band gap leads to a high transmission[8]. Here in our case the band gap has been increased with Al doping which correlate with the literature. At higher doping concentration of aluminum doping, the transmittance decreases which can be attributed to the defects produced by dopant in the host lattice and will increase scattering phenomenon of photon. Conversely, another factor which perhaps presents contribution in the reduction of optical transmission is the free carrier absorption of photons. With heavy doping the free carrier

absorption of photons may possibly turn-down the transmission of the ZnO nanorods [9-10]. The combined graph of all the samples has been shown in the figure 4.6.

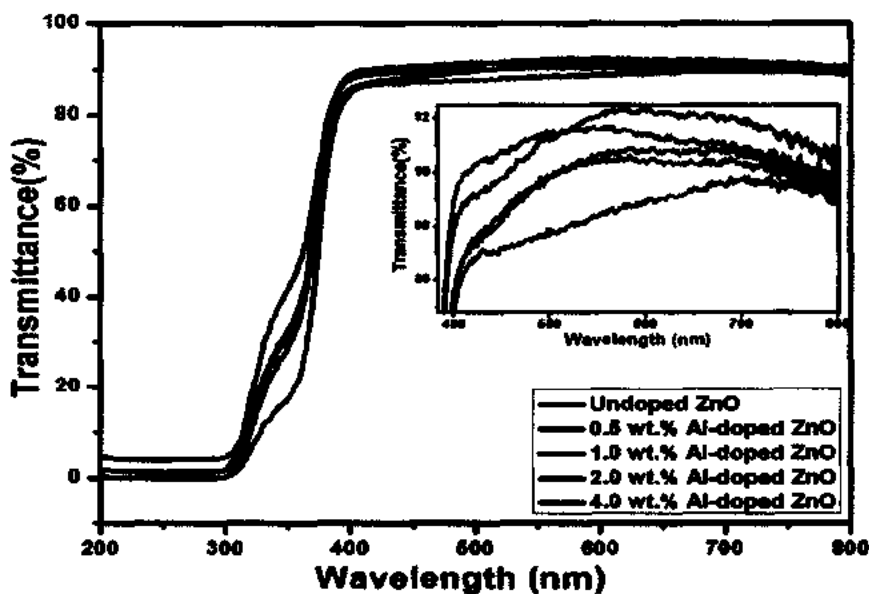


Figure 4.6: Combined optical transmittance graph of Undoped and 0.5 wt.%, 1.0 wt.%, 2.0 wt.%, 4.0wt. % Al-doped ZnO nanorods.

4.3 Optimization of nanorods

SEM was used to analyze the surface morphology of the synthesized Al-doped ZnO nanorods. By varying different growth parameters a series of experiment was performed variety of nanorods was prepared as illustrated in figure 4.7. It shows that the surface morphology and orientation can be control by varying the parameters related to CBD growth mechanism. But it was observed that the effect of seed layer on the orientation of ZnO nanorods leading over all others parameters. Particularly the focus of the present work was to grow well aligned Al-doped ZnO nanorods structure because they provide direct path to the charge carriers from the point of photogeneration to the conducting electrodes in photovoltaic devices [11]. It also decreases the electron recombination rate to some extent. In addition, it is expected that electron transport in single crystalline rod will be more compared to randomly oriented polycrystalline system or disordered structure of nanoparticles. In disordered structure, chances of free electron scattering are greater [12].

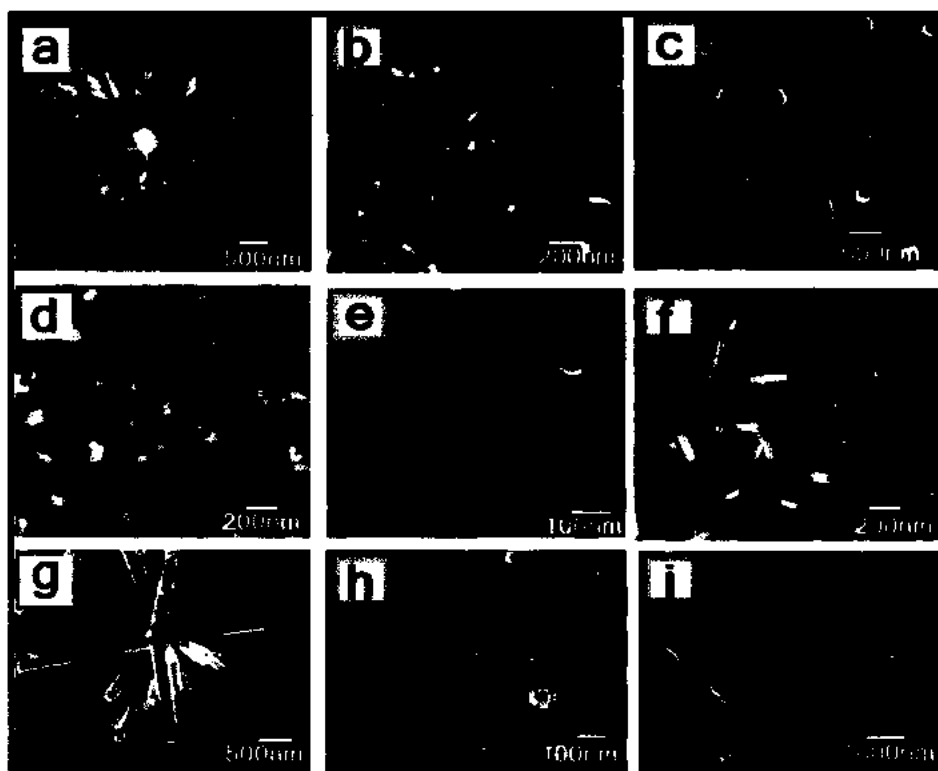


Figure 4.7: Variety of Al-doped ZnO nanorods grown in this project.

The enormous effect of seed layer was studied by SEM technique to scrutinize the surface morphology of Al-doped ZnO nanorods grown on the surface of uncoated, 6 times and 10 times ZnO seed coated glass substrates. The nanorods grown on uncoated substrates were just only for comparison studies. The Scanning electron microscope (SEM) image of Al-doped ZnO nanorods grown on uncoated glass substrate is shown in the figure 4.8. It is cleared from the image that the nanorods have poor morphology because the lengths and diameters of the nanorods are not uniform. The diameter of the nanorods varies from 70nm to 240nm. Also they are not well aligned in the direction perpendicular to the substrate. It may be due to the mismatching lattice structure or the surface of the substrate may not be smooth at nano scale due to which the morphology of nanorods greatly affected. Thus, the nanorods growth is random not properly aligned along the direction perpendicular to the substrate.



Figure 4.8: SEM image of Al-doped ZnO nanorods grown on uncoated glass substrate.

Now to control the alignment and diameter uniformity of Al-doped ZnO nanorods, the substrates were pre-coated 6-times with ZnO seed by spin coating method. In this case both the diameter and alignment of the nanorods were improved extremely. The small variation in the diameter is may be due to the inadequate structure of seed. The Al-doped ZnO nanorods grown on 6-times seed coated glass substrates are shown in figure 4.9.

As from figure the diameter varies from 60nm to 200nm but majority of the nanorods have uniformity in their diameters. The density of the nanorods also improved with seed coating. The small variation in the diameter homogeneity is probably due to the crystal size of the seeds. The nanoparticles of seeds which play the role of nucleation sites influence the diameter of nanorods i.e. uniform nanoparticales results uniform diameter nanorods [8, 13].

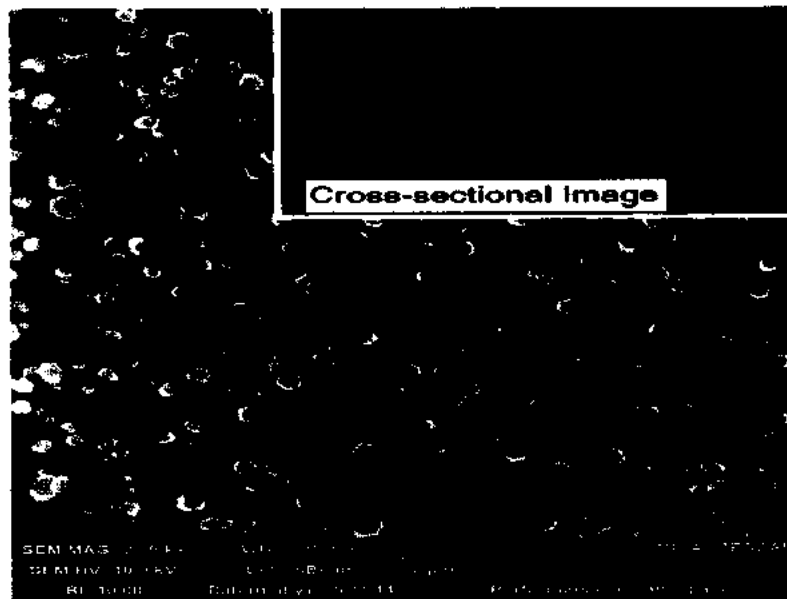


Figure 4.9: SEM image of Al-doped ZnO nanorods grown on ZnO 6-times seed coated glass substrate.

For further improvement in the alignment and to enhance the homogeneity in diameter the Al-doped ZnO nanorods were grown on 10-times fine seed coated substrates as shown in the figure 4.10. This time the SEM results confirm that the nanorods are well aligned and have great extent of homogeneity in diameter distribution. They are grown properly in the direction perpendicular to the substrate surface. Moreover, it is also observed that the density of the nanorods is greater compared to uncoated and 6-times seed coated [14]. Almost, all the nanorods have uniform diameters. As a result a good quality uniform seed layer with appropriate thickness present uniform, high quality aligned and dense nanorods. With the increasing number of seed coatings, the thickness of the seed layer increases which can control the orientation and density of the nanorods growing on it. Besides this, the SEM image also provides the confirmation that the structure of Al-doped ZnO is typical hexagonal. The nanorods show good crystal structure along c-axis.

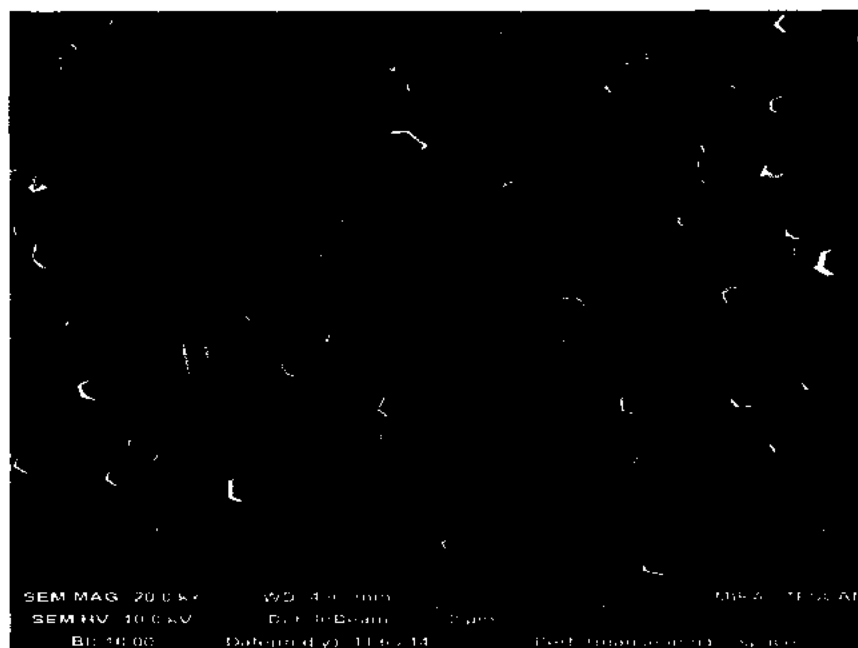


Figure 4.10: SEM image of Al-doped ZnO nanorods grown on 10-times ZnO seed coated glass substrate.

Another effect of fine seed layer on the surface morphology of Al-doped ZnO nanorods is to control the density of nanorods. Heteronucleation on to foreign surfaces take place easily but its controlling is difficult task. The nanoparticles of ZnO seed on the substrate surface act as nuclei for ZnO nanorods and help in their vertical alignment due to the matching lattice structure. But after annealing these nanoparticles either dispersed widely or merges to form bigger island. Then during the growth of ZnO nanorods Zn^{2+} may diffuse only onto the top sites and not troughs among the nanorods. By increasing the number of seed coating, the separation among the nanoparticles decreases and nucleation sites increases which control the density of ZnO nanorods[13]. The number of ZnO nanorods in unite area will be greater if they are grown on the more times seed coated substrates. Al-doped ZnO nanorods grown over uncoated and different times ZnO seed coated glass substrates shown in the figure 4.11. The density of nanorods grown on 12-times seed coated substrate is high then 8-times, 4 times seed coated and uncoated.

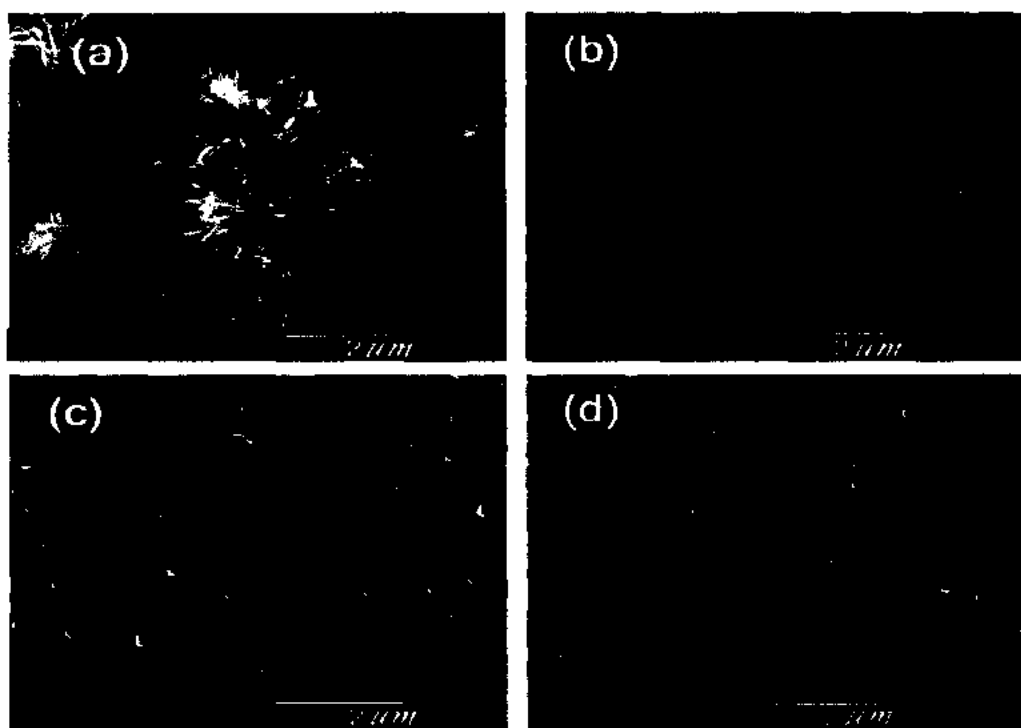


Figure 4.11: Al-doped ZnO nanorods grown on (a) uncoated (b) 4-times (c) 8-times (d) 12-times ZnO seed coated substrates.

4.4 Compositional analysis (EDX)

The quantitative compositional analysis of Al-doped ZnO nanorods was performed by the help of energy dispersive spectroscopy technique. This analysis technique exposed the elemental composition present in the sample and estimates its quantity in the sample. Figure 4.11 exhibits the EDX spectra result of 0.5 wt.% Al-doped ZnO nanorods. It is clearly observed that all the desired elements Zn, O and Al are present. It was also noted that with the increasing doping concentration, the EDX spectra gives increasing value of dopant in wt.% but not in a proper order. The dopant element Al is present with different concentration in the elemental compositional spectra along with Zn and O elements.

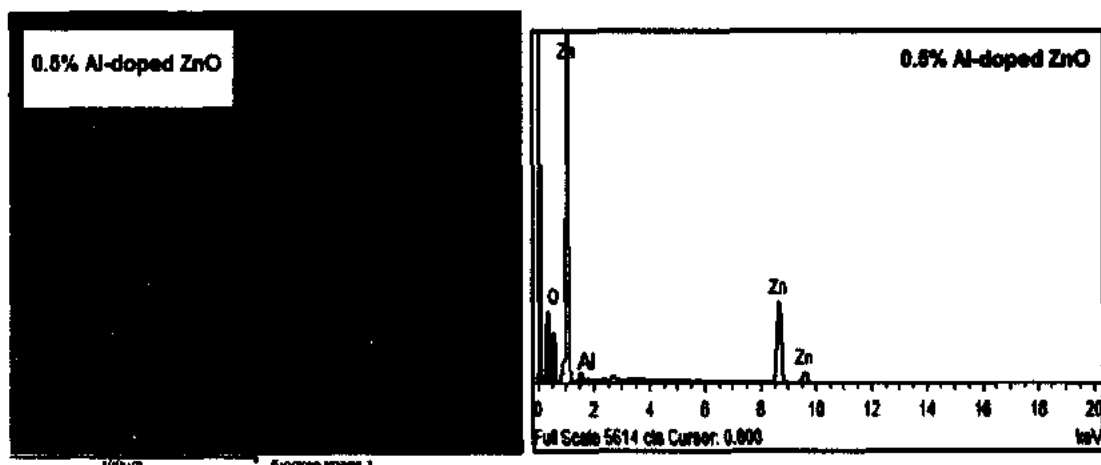


Figure 4.12: EDX spectra of 0.5 wt.% Al-doped ZnO nanorods.

The percentage weight of Aluminum in all Al-doped ZnO nanorods samples was not exactly the same as taken at the time of synthesis. The reason for that might be that some of the aluminum atoms did not reach to the ZnO sites i.e. missing the Zn sites and go to the interstitial sites or settle down in the remaining precipitate. That's why the apparent weight % not equal to the real weight % obtained from the EDS results. At last, the experimental results confirmed the truth of Al-doping into the ZnO nanorods structure.

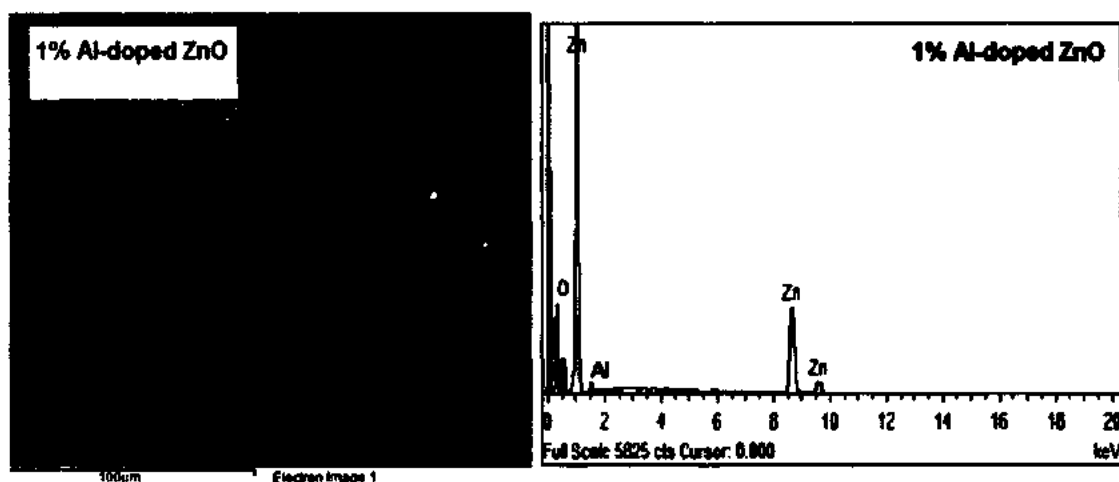


Figure 4.13: EDX spectra of 1 wt.% Al-doped ZnO nanorods.

4.5 Conclusions

In this research work ZnO nanorods were grown by using chemical bath deposition method at low temperature. The XRD measurements illustrated that the as synthesized nanorods possess hexagonal wurtzite crystal structure with (002) preferential growth. With the help of UV/Vis spectroscopy it was substantiated that the fabricated samples show high transmittance in the visible region in the wavelength range of 500nm to 800nm, also the band gap increases with aluminum doping in the ZnO. The EDX provides evidence for the successful doping of Al in ZnO matrix. Furthermore, the morphology/alignment of the nanorod structures is tuned through different experimental conditions. It is shown that by tuning the seed layer, alignment of the nanorods can be controlled. Particularly by changing the number of seed layer coatings the alignment and uniform size distribution has been achieved. This aspect is very essential to control the growth of ZnO nanorods on any substrate. Both the XRD and SEM results consent that the nanorods grown well in the direction perpendicular to the surface of substrate having typical hexagonal wurtzite crystal structure along c-axis. Such type of well oriented Al-doped ZnO nanorods offer greater potential in future photovoltaic devices compared to thin film or randomly oriented ZnO nanostructures.

In future, this research work can be helpful to fabricate ZnO and Al-doped ZnO nanorods based novel devices, such as solar cell, strain sensor and nanogenerator to change the future life style.

References

- [1] D. Wu, Z. Haung, G. Yin, Y. Yao, X. Liao, D. Han, X. Huang, J.Gu, *Cryst. Eng.Comm.* **12**, 192 (2010).
- [2] P. S. Kumar, S. M. Maniam, J. Sundaramurthy, J. Arokiaraj, D. Mangalaraj, D. Rajarathnam, M. P. Srinivasan, L. K. Jian, *Materials Chemistry and Physics* **133(1)**, 126 (2012).
- [3] S. Yun, J. Lee, J. Chung, S. Lim, *Journal of Physics and Chemistry of Solids*, **71**, 1724 (2010).
- [4] B. D. Cullity, *Elements of X-ray diffractions*, Addison-Wesley, MA, 102 (1978).
- [5] R.A. Smith, *Semiconductors*, 2nd ed., Cambridge University Press, Cambridge, (1978).
- [6] J.Torrent, V. Barron, *Encyclopedia of Surface and Colloid Science*, Mercei Dekker, Inc, New York, (2002).
- [7] J. I. Pankove, *Optical processes in semiconductor*, Prentice-Hall, Englewood Cliffs, (1971).
- [8] C. H. Hsu, D. H. Chen, *Synthesis and conductivity enhancement of Al-doped ZnO nanorods array thin film*, *J. Nanotechnology* **21**, 285603 (2010).
- [9] B. Joseph, P.K. Manoj, V.K. Vaidyan, *Ceram. Int.* **32**, 487(2006).
- [10] B. Ergin, E. Ketenci, F. Atay, *Int. J. Hydrogen Energy*, 1(2008).
- [11] B. J, Koppa, R. F. Davis, R. J. Nemanich, *Applied Physics Letters*, **82**, 400(2003).
- [12] M. Guo, P. Diao, S. Cai. *Journal of Solid State Chemistry* **178 (6)**, 1864 (2005).
- [13] T. Ma, M. Guo, M. Zhang, Y. Zhang, X. Wang. *Nanotechnology* **18 (3)**,0356051 (2007).
- [14] S.Yun, J. Lee, J. Yang, S. Lim, *Physica B*, **405**, 423 (2010).